

Phenomenological and Molecular Theories of Dielectric and Electrical Relaxation of Materials

Graham Williams and Dale K. Thomas
Department of Chemistry, University of Wales Swansea, Singleton Park,
Swansea SA2 8PP, UK.

1. INTRODUCTION

The interaction of electromagnetic radiation with matter is of fundamental importance in basic and applied science. Ask any scientist about this subject and it is likely that he/she will tell you that this is 'spectroscopy' and will go on to explain how quantised vibrations, quantised rotational and electronic transitions for atoms, molecules or whole materials give rise to IR and UV/visible absorption and emission spectra. If it is pointed out that such spectra are observed for frequencies greater than $\sim 3 \times 10^{11}$ Hz, so what happens in the remaining frequency range 10^{11} Hz down to 10^{-6} Hz ?, a blank response is often obtained or some may mention the microwave spectroscopy of gases where pure quantised rotational or inversion spectra (eg as for ammonia) may be observed. I make this point to emphasize that it is not generally appreciated that spectroscopic dispersion of dielectric permittivity (and hence refractive index) and associated energy absorption regions may be observed for a material over the entire range from 10^{11} Hz to 10^{-6} Hz due to classical electric *polarization* and electrical *conduction* processes. The magnitude of the effects and the frequency location of the energy absorption features associated with these processes will depend markedly upon the chemical and physical nature of a material and the temperature and pressure at which it is studied. Studies of electric polarization and conduction processes are made under the titles 'Dielectric Relaxation Spectroscopy' (DRS), 'Impedance Spectroscopy' (IS), 'Electrical Impedance Spectroscopy' (EIS) or 'Electrical Relaxation Spectroscopy' (ERS). This diversity of description is historical and arose because studies were made for different reasons with different classes of materials, usually by scientists from different backgrounds e.g. in physical chemistry, condensed-matter physics, electronic physics, materials science, polymer science, solid-state physics etc.. For example, many use DRS as an investigative tool for the study of molecular motions of dipolar molecules in liquids and solids. The variation of complex dielectric permittivity with frequency will, as we shall see below, give information on the natural rotational diffusional motions of dipolar molecules in a material in the absence of an applied electric field. Others use DRS, EIS, IS, ERS to study hopping conduction of charged species in polar solids and semi conductors. The whole subject of electrical conduction and photoinduced-conduction in solids is included under these headings so the subject is wide-ranging. The variation of electrical conductivity with measuring frequency may, as we shall see below, give information on the natural translational diffusional motions of ions in a material in the absence of an applied field.

The electrical/dielectric properties of materials, as determined by DRS, IS, EIS, ERS, may be expressed in different ways, and this has led to some confusion and to different ways of interpreting the same basic data. Rather than being regarded as one subject, namely, '*the frequency-dependent electrical/dielectric properties of materials*', DRS, IS, EIS and ERS studies of different classes of materials have developed along parallel lines with limited overlap, even though they use the same measurement techniques and instrumentation. In this article, we give an introductory account of selected topics that are essential to an understanding and application of the electrical/dielectric studies of materials. The account is intended to aid a person entering the field in understanding the different quantities that are measured experimentally, how they are inter-related and how, in model cases, they may be related to molecular processes involving the rotational motions of dipolar species and the translational motions of charged species. Appropriate references are given where more

detailed accounts of the macroscopic and molecular theories of electric polarization and conduction will be found.

Studies of the electrical/dielectric (E/D say) properties of materials, reported as DRS, IS, EIS and ERS data, have been made increasingly over the past ten years. For DRS studies, the experimental quantity is the complex dielectric permittivity $\epsilon(\omega)$ defined as

$$\epsilon(\omega) = \epsilon'(\omega) - i\epsilon''(\omega) \quad (1)$$

where $\omega = 2\pi f/\text{Hz}$, ϵ' is the real permittivity and ϵ'' is the dielectric loss factor. For liquids and solids containing molecular dipoles that have rotational freedom $\epsilon(\omega)$ may be related to $\langle \mu^2 \rangle$, the mean squared dipole moment per molecule, and to the Fourier transform of a time-correlation function $\Phi_{\mu}(t)$ for the reorientational motions of the dipoles, as will be explained below. Thus, DRS provides a means of determining the average rate of molecular tumbling motions in different materials (eg dipolar liquids, rotator-phase molecular crystals, amorphous, crystalline and liquid-crystalline solid polymers). Such DRS studies are complementary to those using nuclear magnetic resonance (NMR) relaxation, dynamic mechanical thermal analysis (DMTA), quasi-elastic light scattering (QELS), quasi-elastic neutron scattering (QENS) and transient fluorescence depolarization techniques. While those techniques advanced markedly from the 1950s to the 1990s in terms of (i) instrumentation (ii) underlying theory and (iii) applications to different materials, the older technique of DRS made slower progress due to the difficulty of making accurate measurements quickly and efficiently over such a large f-range (10^{-6} to 10^{11} Hz). During the past ten years or so, the situation has changed remarkably with the advent of modern dielectric spectrometers that are able, individually, to cover wide bands within the overall range. Thus, for example, Novocontrol spectrometers are available for the ranges 10^{-6} to 10^7 Hz, 10^6 - 10^9 Hz and to higher frequencies in the microwave range. These spectrometers are able to make accurate DRS measurements of $\epsilon(\omega)$ and hence related electrical/dielectric quantities (see below) of materials in an automatic, pre-programmed manner, quickly and efficiently. In addition, these data may be fitted to empirical and molecular relaxation/correlation time-functions or frequency functions using specialised software, thus allowing DRS spectra to be characterised over a very wide f-range. The same conclusion applies to IS, EIS and ERS studies that use the same instrumentation but present the electrical/dielectric properties in terms of complex electrical impedance $Z(\omega)$, complex electrical admittance $Y(\omega)$, complex electric modulus $M(\omega)$ or complex electrical conductivity $\sigma(\omega)$.

Before we describe details of the theory underpinning DRS, IS, EIS and ERS studies it is worth noting that the electrical/dielectric behaviour of materials pervades modern science and technology as illustrated by:-

- dielectric relaxation of organic materials including polymers
- electronic conduction of inorganic and organic materials, including semiconductors
- electrical conduction, by ion-motions, of conventional electrolytes, polyelectrolytes and novel electrolytes, including salt/polymer complexes
- electrical insulation in cables and capacitors using polymers (eg polyethylene, polypropylene, polystyrene, polytetrafluoroethylene, polyvinyl chloride)
- piezoelectric, pyroelectric and ferroelectric behaviour of inorganic materials (eg barium titanate) and organic materials (eg polyvinylidene difluoride)
- UHF and microwave dielectric heating of materials, used for domestic cooking, industrial food processing and microwave dielectric heating of reaction mixtures.

2. DIELECTRIC AND RELATED ELECTRICAL STUDIES

2.1. Literature

DRS is a mature subject in terms of experimental techniques, the theory of electric polarization and conduction phenomena in organic and inorganic liquids and solids and the experimental data for such materials. Key references to the subject are as follows:-

- Experimental techniques, theory and experimental results for low molar mass materials - the texts of Smyth [1], Hill, Vaughan, Price and Davies [2], Bordewijk and Böttcher [3].
- Experimental techniques, theory and experimental results for polymer materials - the texts of McCrum, Read and Williams [4], Blythe [5] and, very recently the text edited by Runt and Fitzgerald [6].

- Experimental techniques, theory and experimental results for ionic crystals - the text by Nowick and Berry [7] and the reviews by West [8-10], and for glass-forming materials, including molten salts, - the text by Wong and Angell [11] and the key papers by Moynihan and coworkers [12-15]. Note: ref. 13 and 15 contain key references to the electrical conduction behaviour of ionic materials.

Pochan, Fitzgerald and Williams [16] have reviewed the experimental techniques used for the DRS of polymers, while the original texts of Von Hippel [17, 18] remain the classic accounts of the phenomenological theory of electric polarization and conduction processes and the early applications of dielectric materials. The dielectric properties of materials, especially polymers, including experiment and theory, have been the subject of a series of updated reviews by the author [19-29].

In the majority of DRS studies of materials, molecular relaxation processes, due to the motion of dipole groups as whole molecules or as chain segments in polymer molecules, are observed as multiple dielectric loss peaks in plots of $\epsilon''(\omega)$ -vs- $\log(f/\text{Hz})$. In addition, at low frequencies an increasing loss with decreasing frequency is observed due to charge-conduction and electrode polarization in a material, giving information on the apparent translational diffusion coefficient of the mobile charges (ions or electrons), as we shall see below. The questions arise - (i) what presentational forms should electrical/dielectric properties take and (ii) how may they be interpreted using phenomenological theories and using molecular theories for the rotational and translational motions of molecular species? These questions will be addressed below.

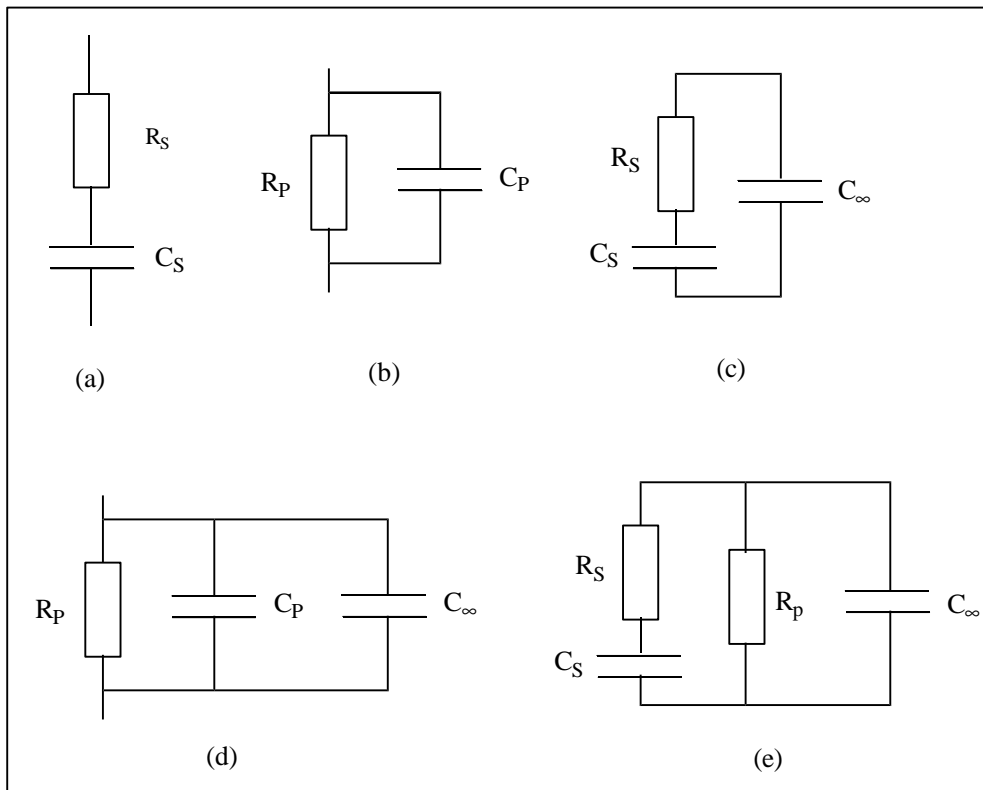


Figure 1. Model equivalent electrical circuits for relaxation and conduction as described in the text.

2.2. Extensive Experimental Quantities

For frequencies below 10^8 Hz, it is convenient to use equivalent electrical circuits made up of resistors, capacitors and, where appropriate, inductors to represent the electrical/dielectric (E/D) properties of a material. This 'lumped circuit' representation has been widely-used, especially in the IS and IRS studies of ionic materials [8-10]. The measuring instrument (eg an impedance analyzer) will measure a sample in a parallel plate or coaxial dielectric cell as either

- (a) a resistor R_S in series with a capacitor C_S (fig. 1(a))

or

(b) a resistor R_p in parallel with a capacitor C_p (fig. 1(b)).

For a.c. measurements these electrical circuits can be forced to be equivalent, giving the following equations for the electrical admittance $Y(\omega)$ and the electrical impedance $Z(\omega)$

$$Y(\omega) = \frac{1}{Z(\omega)} = G_p(\omega) + i\omega C_p(\omega) = \frac{1}{R_s(\omega) + 1/i\omega C_s(\omega)} \quad (2)$$

where the parallel conductance $G_p(\omega) = R_p(\omega)^{-1}$ and, in general, G_p , C_p , R_s and C_s vary with frequency $f = \omega / 2\pi$ for a material. The following relations are obtained from eqn. (2).

$$C_s(\omega) = C_p(\omega) [1 + D^2]; \quad G_p(\omega) = \frac{1}{R_p(\omega)} = \frac{D^2}{R_s(1 + D^2)} \quad (3a, 3b)$$

$$D(\omega) = \omega R_s(\omega) C_s(\omega) = [\omega R_p(\omega) C_p(\omega)]^{-1} \quad (3c)$$

Where $D_p(\omega)$ is known as the *dissipation factor*.

If a real material is thought to correspond to a particular equivalent electrical circuit then the resistor and capacitor elements defined in that circuit should be independent of frequency. For example, a dielectric material having no relaxation behaviour but possessing a steady dc conductance due to ion-motions should be regarded as a capacitance C_p in parallel with a conductance R_p (see fig. 1(b)), whose values are independent of frequency in eqn. (2) above. In consequence, the forced-equivalent circuit of $R_s(\omega)$ in series with $C_s(\omega)$ (see eqn. (2)) gives $R_s(\omega)$ and $C_s(\omega)$ as f-dependent quantities whose values are obtainable in using $[R_p, C_p]$ in eqns. (3) and (4) above. It is important to emphasize that the forced equivalence in eqns. (2) for series and parallel circuits applies only to a.c. measurements and does *not* extend to measurements made in the time-domain as the step-on and step-off response (charge or current) to an applied voltage V . The series circuit $[R_s, C_s]$, fig. 1(a) where R_s and C_s are constant, acts as a 'relaxing' element with step-on and step-off responses for the transient current $I(t)$ following the step-application and withdrawal of a voltage V being given, respectively, by

$$I_{on}(t) = (V/R_s)[1 - \exp(-t/\tau_{RC})] \quad (4a)$$

$$I_{off}(t) = (V/R_s)\exp(-t/\tau_{RC}) \quad (4b)$$

where $\tau_{RC} = R_s C_s$. In the step-on experiment for $t \rightarrow \infty$ the capacitor is charged but the circuit does not draw a current. The parallel circuit $[R_p, C_p]$, where R_p and C_p are constant, acts as a 'dissipating' element at all times for a step-on voltage since for the the capacitor charges as a δ -function with time and the resistor draws a steady current $I_{on}(t) = (V/R_p)$. It should be evident from this that the forced equivalence of series and parallel circuits (eqn. (2)) for a.c. experiments does not apply to d.c. step-function experiments. A further point to emphasize is that it may be fundamentally incorrect to represent a dielectric material in terms of an equivalent circuit of resistors and capacitors having f-independent values. For example, for a material in which, under step-on dc-voltage conditions, charged species migrate but are not electrically-neutralized at the electrodes then a blocking capacitative layer builds up with time at the electrodes. At long times the charging current $I_{on}(t)$ will cease to flow and the material stores energy in the capacitor plus blocking layer as if it were a polarized material in the presence of the steady voltage. Since the blocking layer did not exist in the absence of the voltage it seems inappropriate to represent the system as a lumped circuit having a series arrangement of sample capacitance and a blocking layer capacitance. If a mathematical model can be given for the establishment of the blocking layer with time then $I_{on}(t)$ may be calculated without recourse to equivalent lumped circuits. Note also that for this example removal of the steady voltage will not necessarily lead to a decay of $I_{off}(t)$ with time that mirrors $I_{on}(t)$, so linear response is not obtained, generally, and Fourier transformation of $I_{off}(t)$ to give predictions of the a.c. behaviour of the circuit is not possible. Such considerations are usually not made, and the effects of electrode polarization need further theoretical modelling at this time.

To conclude this Section, we note that a dielectric material can be measured at frequencies below $\sim 10^6$ Hz as $[R_s, C_s]$ or $[R_p, C_p]$ equivalent circuits where these components are, in general, frequency-dependent.

2.3. Intensive Experimental Quantities

The measured values of $Y(\omega) = Z(\omega)^{-1}$ will depend on the geometry of a sample (sample area A and thickness d for a parallel-plate cell) so it is necessary to express the electrical/dielectric (E/D) properties of a material in terms of intensive quantities, which are:- dielectric permittivity relative to vacuum $\epsilon(\omega)$, electrical modulus $M(\omega) = \epsilon(\omega)^{-1}$ and electrical conductivity $\sigma(\omega)$. If the empty dielectric cell has a geometrical capacitance given by $C_o = A\epsilon_v/d$, where ϵ_v is the permittivity of free space, then

$$\epsilon(\omega) = \frac{Y(\omega)}{i\omega C_o} = \frac{1}{i\omega C_o Z(\omega)} \quad (5a)$$

$$M(\omega) = \frac{i\omega C_o}{Y(\omega)} = i\omega C_o Z(\omega) \quad (5b)$$

where $\epsilon(\omega) = \epsilon'(\omega) - i \epsilon''(\omega)$ and $M(\omega) = M'(\omega) + i M''(\omega)$.

The inter-relationships between ϵ , M and σ are expressed as follows:

$$\epsilon(\omega) = \frac{1}{M(\omega)} = \frac{\sigma(\omega)}{i\omega\epsilon_v} \quad (6)$$

where $\sigma(\omega) = \sigma'(\omega) + i \sigma''(\omega)$. From eqns. (5) and (6) we see that the same E/D data may be presented as the extensive quantities $Y(\omega)$ or $Z(\omega)$ or as the intensive quantities $\epsilon(\omega)$, $M(\omega)$ or $\sigma(\omega)$. In practice, experimental data for materials are frequently presented in any one of these five different representations. Data from DRS studies of materials are usually presented as $\epsilon(\omega)$ [1-4] and sometimes as $M(\omega)$ and $Z(\omega)$. IS, EIS and ERS data for materials are usually presented as $Z(\omega)$ or $M(\omega)$ and occasionally as both [8-10, 12-16]. The particular presentation is chosen to emphasize the process under investigation. Thus, for DRS studies of molecular motions of dipolar molecules in the liquid and solid states $\epsilon(\omega)$ is chosen and exhibits dispersion of $\epsilon'(\omega)$ with increasing frequency accompanied by a loss peak for $\epsilon''(\omega)$. We shall see below that this is a particularly useful representation since inverse Fourier transformation of $\epsilon''(\omega)$ gives information on the time-correlation function (TCF) for the motions of the dipoles. For IS, EIS, ERS studies of ionically-conducting materials (eg molten salts), $M(\omega)$ is often chosen and is found to exhibit dispersion of $M'(\omega)$ and a loss peak for $M''(\omega)$. It will become apparent that it is not obvious how $M(\omega)$ may be related to TCF for the translational motions of the charged species and that $\sigma(\omega)$ would be the preferred quantity to represent the behaviour of conducting materials.

In recent years there had been a marked increase in the number of DRS, IS, ERS studies of polarization and conducting processes in glass-forming liquids, ionic liquids, polymers (amorphous, crystalline, liquid-crystalline), ionic crystals, liquid crystals, and chemically-reacting systems (eg epoxide-amine polymerizing systems). An excellent source of experimental data together with their theoretical interpretations is to be found in the published records of the Crete and Alicante Conferences organised by Ngai, Wright, Riande, Bello and their associates [30, 31]. The numerous papers in those published volumes show how $Z(\omega)$, $\epsilon(\omega)$, $M(\omega)$ and $\sigma(\omega)$ are all used to present E/D data for such materials.

3. MODEL LUMPED CIRCUITS

We consider simple equivalent circuits for samples that exhibit dielectric relaxation and electrical conduction and obtain relations for different E/D quantities.

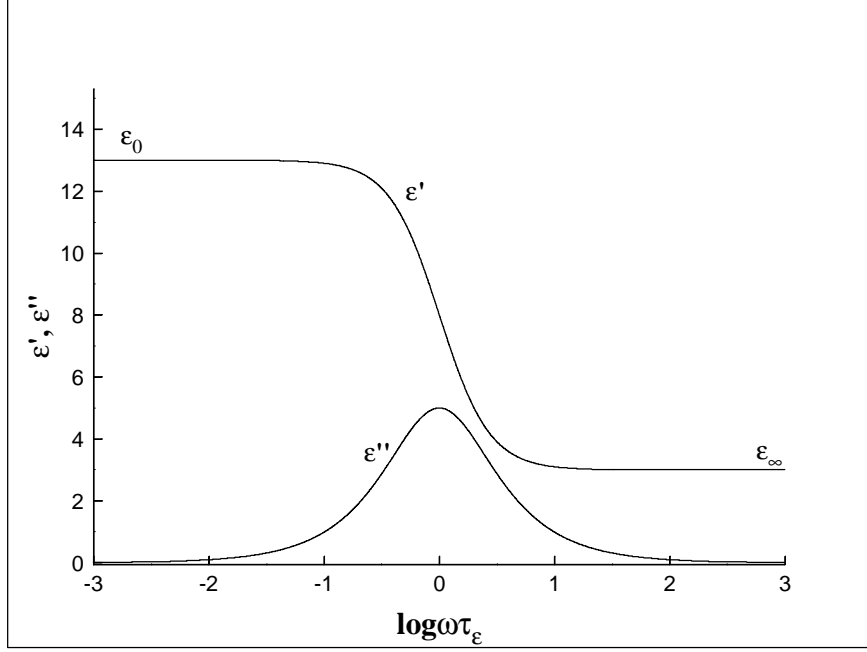


Figure 2. Plots of real permittivity ϵ' and loss permittivity ϵ'' -vs- $\log \omega\tau_\epsilon$ for a sample represented as the equivalent circuit fig. 1(c) with chosen values of ϵ_0 and ϵ_∞ .

3.1. Relaxation

Consider a parallel-plate capacitor of area A and plate-separation d to contain a dielectric material that exhibits relaxation. The equivalent circuit is a series pair $[R_s, C_s]$ in parallel with a capacitance C_∞ where all components have f -independent values (see figure 1(c)). We write

$$Y(\omega) = i\omega C_0 \epsilon(\omega) = i\omega C_\infty + \frac{1}{R_s - i/\omega C_s} \quad (7)$$

where $C_0 = A\epsilon_v/d$ is the geometric inter-electrode capacitance of the cell and ϵ_v is the permittivity of a vacuum. Writing $\epsilon_\infty = C_\infty/C_0$ and $\tau_{RC} = R_s C_s$, we obtain

$$\epsilon(\omega) = \epsilon_\infty + \frac{\epsilon_0 - \epsilon_\infty}{1 + i\omega\tau_{RC}} \quad (8)$$

where $\epsilon_0 - \epsilon_\infty = C_s/C_0$. Eqn. (8) shows that the circuit exhibits relaxation behaviour as follows: From eqn. (8) we write

$$\epsilon'(\omega) = \epsilon_\infty + \frac{(\epsilon_0 - \epsilon_\infty)}{1 + \omega^2\tau_{RC}^2} \quad \epsilon''(\omega) = \frac{(\epsilon_0 - \epsilon_\infty)\omega\tau_{RC}}{1 + \omega^2\tau_{RC}^2} \quad (9a, 9b)$$

Fig. 2 shows plots of $\epsilon'(\omega)$ and $\epsilon''(\omega)$ -vs- $\log \omega\tau_\epsilon$ for ϵ_0 and ϵ_∞ values chosen arbitrarily as 13 and 3 respectively and for $\tau_\epsilon = \tau_{RC} = 1$ sec. $\epsilon'(\omega)$ falls with increasing frequency and $\epsilon''(\omega)$ shows a peak at $\omega_m \tau_{RC} = 1$. The peak height is $(\epsilon_0 - \epsilon_\infty)/2$ and the 'relaxation strength' is $(\epsilon_0 - \epsilon_\infty)$. The area below the plot of ϵ'' -vs- $\log_e \omega\tau_\epsilon$ is given by $(\epsilon_0 - \epsilon_\infty) \pi/2$, so the total relaxation strength, as given by this area, is directly related to the magnitude of the dielectric dispersion $\epsilon_0 - \epsilon_\infty$. For real dielectric materials the same is true for a 'single relaxation time process', as we shall discuss below.

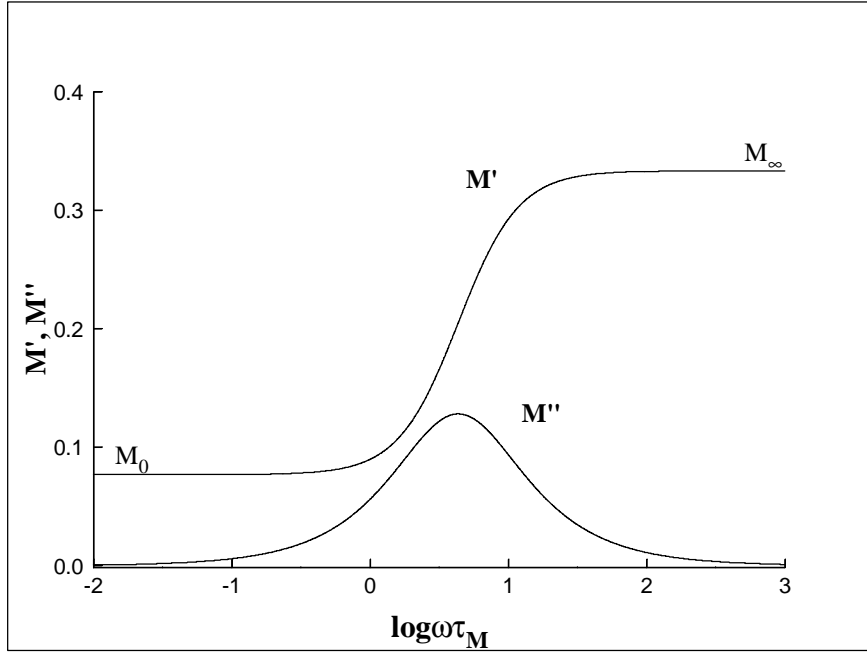


Figure 3. Plots of the real electrical modulus M' and the loss modulus M'' vs- $\log \omega\tau_M$ as derived from the data of figure 2.

In the mechanical relaxation of solids, materials are often represented in terms of equivalent circuits in which the basic elements are springs (elastic elements) and 'dash-pots' (dissipative elements). The relaxation behaviour is expressed using complex moduli (shear modulus $G(\omega)$ for example) or its inverse, known as the corresponding compliance $J(\omega)$, as is described by Ferry [32] and by McCrum, Read and Williams [4]. Thus mechanical properties can be expressed alternatively as mechanical relaxation $G(\omega)$ or retardation $J(\omega) = G(\omega)^{-1}$ for a viscoelastic material. By analogy the modulus representation of electrical properties is sometimes used in electrical studies [12-15]. For the electrical circuit given in fig. 1(c) it follows that $M(\omega)$ is given by

$$M(\omega) = M'(\omega) + i M''(\omega) = M_\infty + \frac{M_0 - M_\infty}{1 + i\omega\tau_m} \quad (10)$$

where $M_0 = \epsilon_0^{-1}$, $M_\infty = \epsilon_\infty^{-1}$, and $\tau_M = (\epsilon_\infty/\epsilon_0)\tau_\epsilon$. It follows from eqn. (10) that M' rises from $\epsilon_0^{-1} = M_0$ to $\epsilon_\infty^{-1} = M_\infty$ with increasing frequency and M'' gives a bell shaped curve that peaks at $\omega_m\tau_m = 1$, as shown in fig. 3. Thus changing the presentation of data from ϵ to M shifts the absorption peak to higher frequencies (since $\tau_M < \tau_\epsilon$). Finally, we note for the conductivity representation that

$$\begin{aligned} \sigma(\omega) = i\omega \epsilon(\omega) = \sigma'(\omega) + i \sigma''(\omega) = \\ \frac{(\epsilon_0 - \epsilon_\infty)\omega^2\tau_{RC}}{1 + \omega^2\tau_{RC}^2} + i\omega \left[\epsilon_\infty + \frac{\epsilon_0 - \epsilon_\infty}{1 + \omega^2\tau_{RC}^2} \right] \quad (11) \end{aligned}$$

So σ' (ω) increases with increasing frequency to a limiting value $(\epsilon_0 - \epsilon_\infty)/\tau_{RC} = (R_s C_0)^{-1}$ and σ'' (ω) shows a peak. There is no advantage in representing the E/D behaviour of this equivalent circuit as $\sigma(\omega)$. We see that different representations of the E/D behaviour of this simple electrical circuit give very different 'fingerprint' spectra in the f -domain. The preferred representation in this case is as $\epsilon(\omega)$ which gives the relaxation parameters ϵ_0 , ϵ_∞ and τ_{RC} in a simple, direct manner (see eqns. (8) and (9) and fig. 2).

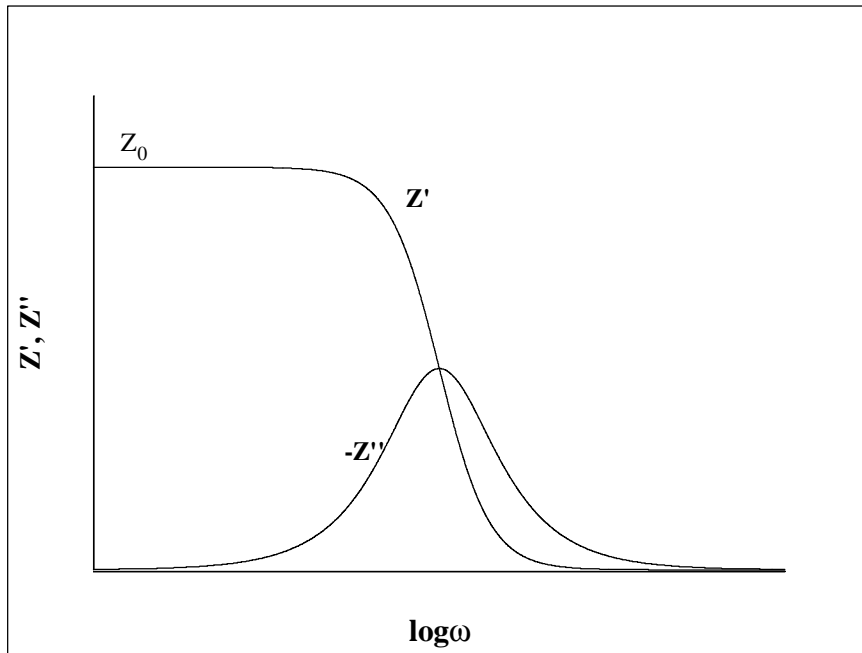


Figure 4. Schematic plots of real impedance Z' and imaginary impedance Z'' -vs- $\log \omega$ for a sample represented as the equivalent circuit fig. 1(d).

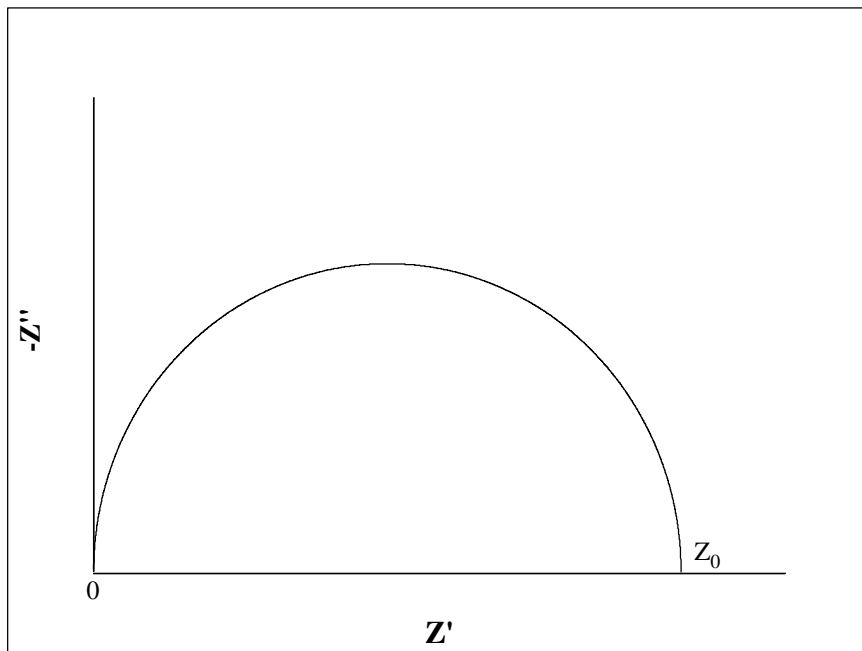


Figure 5. The Argand diagram for the impedance behaviour shown in fig. 4.

3.2. Conduction

Consider a parallel-plate capacitor of area A and plate-separation d to contain a dielectric material that exhibits conduction due to charged species. A suitable equivalent circuit is a parallel pair $[R_p, C_p]$ in parallel with a further capacitor C_∞ where all components have f -independent values (see fig. 1(d)). We write

$$Z(\omega) = (G_p + i\omega C'_p)^{-1} = \frac{R_p}{1 + i\omega\tau'_{RC}} \quad (12)$$

where $C'_p = C_p + C_\infty$ and $\tau'_{RC} = R_p C'_p$

Fig. 4 shows plots of $Z'(\omega)$ and $Z''(\omega)$ -vs- $\log\omega$, where Z' is seen to exhibit a dispersion, falling from $Z(0) = R_p$ to zero while Z'' exhibits a peak at $\omega_m \tau'_{RC} = 1$ with $Z''_{\max} = R_p/2$. The Argand diagram is a semi-circle as shown in Fig. 5.

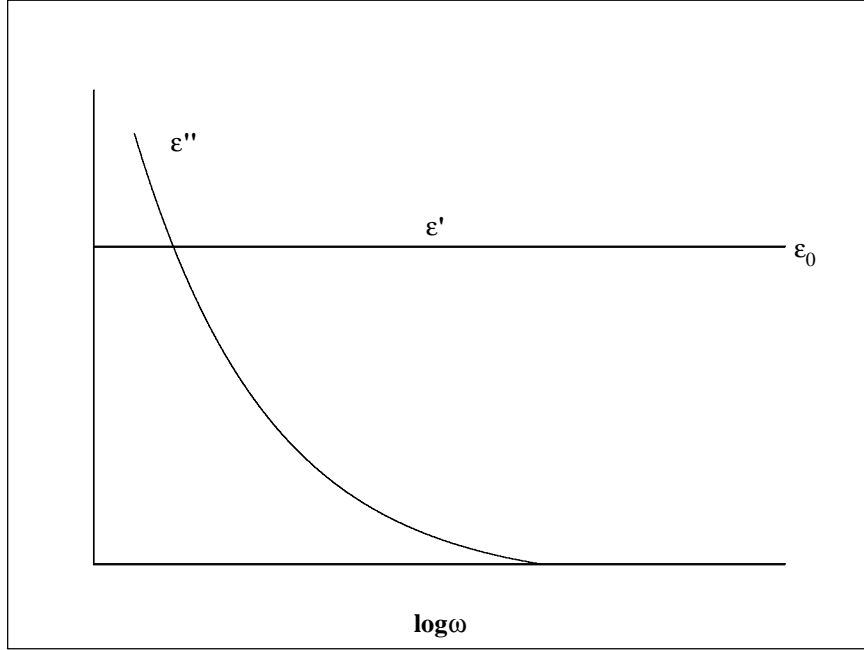


Figure 6. Schematic plots of ϵ' and ϵ'' -vs- $\log \omega$ for a sample represented as the equivalent circuit fig. 1(d).

The expression for $\epsilon(\omega)$ for the parallel $[R_p, C'_p]$ circuit is

$$\epsilon(\omega) = \epsilon'(\omega) - i\epsilon''(\omega) = \epsilon_0 - i[\omega R_p C'_p]^{-1} \quad (13)$$

where $\epsilon_0 = C'_p/C_0$. So ϵ' is independent of frequency and ϵ'' decreases monotonically with increasing frequency as shown in fig. 6. The frequency-independent specific conductivity is given by $\sigma_0 = \epsilon_v(R_p C'_p)^{-1}$. Similarly $\sigma(\omega)$ is written as

$$\sigma(\omega) = \sigma'(\omega) + i\sigma''(\omega) = \sigma_0 + i\omega\epsilon_0\epsilon_v \quad (14)$$

So, $\sigma'(\omega)$ is independent of frequency and $\sigma''(\omega)$ increases with increasing frequency, as shown in fig. 7. Finally, $M(\omega)$ is given by

$$M(\omega) = M_\infty \frac{i\omega\tau_M}{1 + i\omega\tau_M} \quad (15)$$

where $M_\infty = (C_0/C'_p) = 1/\epsilon_0 = 1/\epsilon_\infty$ in this case. So, as in fig. 3, M' increases from zero to $M_\infty = 1/\epsilon_\infty$ with increasing frequency and M'' shows a peak at $\omega_m\tau_M = 1$ with $M''_{\max} = M_\infty/2$. Therefore, M'' follows the single relaxation time expression giving a value for $\tau_M = R_p C'_p$.

Although the parallel $[R_p, C'_p]$ circuit does not exhibit a relaxation response in the time-domain to a step-applied field (the capacitor charges as a δ -response and the resistor passes a steady current) the ac behaviour expressed as $Z(\omega)$ or $M(\omega)$ appears to exhibit relaxation behaviour, as we have seen in figs. 3-5.

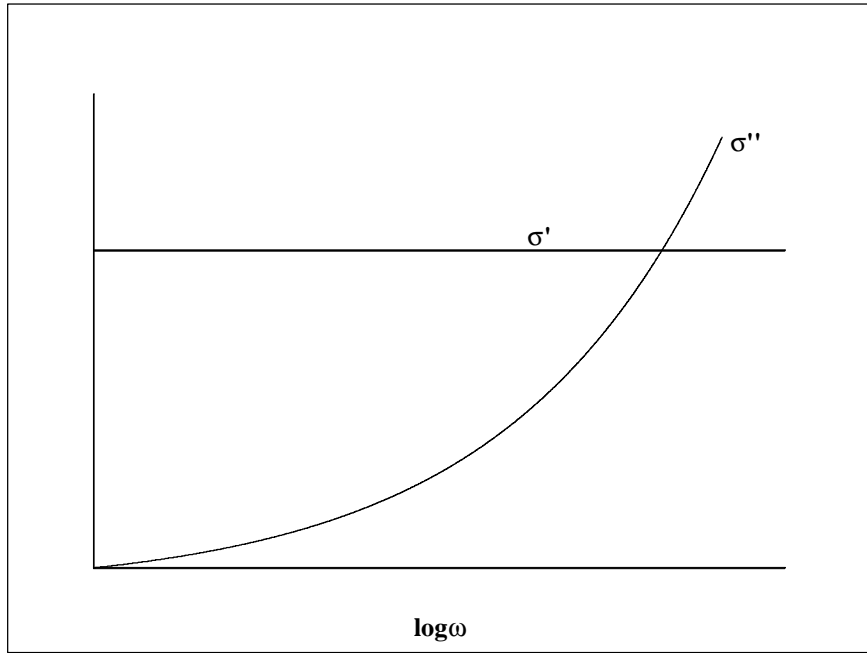


Figure 7. Schematic plots of real conductivity σ' and imaginary conductivity σ'' -vs- $\log \omega$ for a sample represented as the equivalent circuit fig. 1(d).

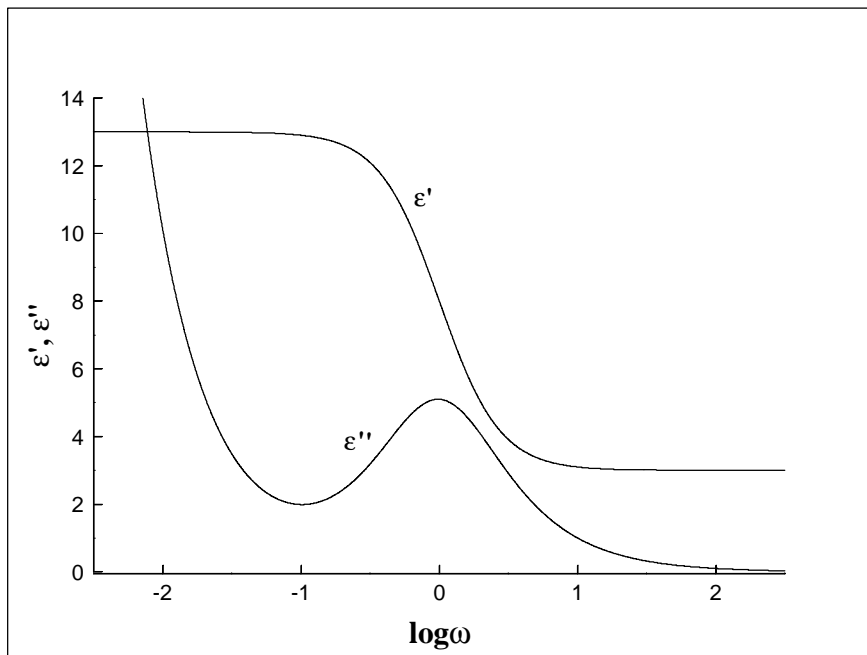


Figure 8. Schematic plots of ϵ' and ϵ'' -vs- $\log \omega$ for a sample represented as the equivalent circuit fig. 1(e), thus exhibiting relaxation and conduction behaviour.

3.3. Relaxation and Conduction

For a material that exhibits relaxation and conduction, one approach is to combine the equivalent circuits shown in figs. 1(a) and 1(d) as shown in fig. 1(e) where C_p has been replaced by $[R_s, C_s]$. We may write

$$\epsilon(\omega) = \epsilon_{\infty} + \frac{\epsilon_o - \epsilon_{oo}}{1 + i\omega\tau_{RC}} - \frac{i}{\omega C_o R_p} \quad (16)$$

where $(\epsilon_0 - \epsilon_\infty) = (C_s/C_\infty)$ and $\tau_{RC} = R_s C_s$.

In fig. 8, we show the resultant plots of $\mathcal{E}'(\omega)$ and $\mathcal{E}''(\omega)$ -vs- $\log \omega$. Dielectric relaxation is observed as in fig. 2, while the conduction process appears as an increasing loss to low frequencies, yielding a value for $C_0 R_p = \epsilon_v \sigma_0^{-1}$. If the form of presentation is changed to $M(\omega)$ we have a complicated equation for $M(\omega)$, depending upon the values for the components, which can yield two apparent relaxation regions, the lower frequency region being associated with a conduction process and the higher frequency region being associated with the relaxation process. The effect of conductivity may be highly suppressed when the data of fig. 8 are presented as $[M', M'']$ as shown in fig. 9. The dispersion and absorption feature due to conduction is seen as a small feature at low frequencies (see also fig. 3). Data for this model circuit, fig. 1(e), presented as $\sigma(\omega)$ show that $\sigma'(\omega)$ at low frequencies is independent of frequency at the value $\sigma_0 = \epsilon_v (R_p C_0)^{-1}$ while $\sigma''(\omega)$ first increases then decreases with increasing frequency. Data presented as $Z(\omega)$ will emphasize the conduction process, and will give, in practice, curves of the form of figs. 4 and 5 with the relaxation process $[R_s, C_s]$ normally being a small feature at frequencies higher than that for the peak in Z'' .

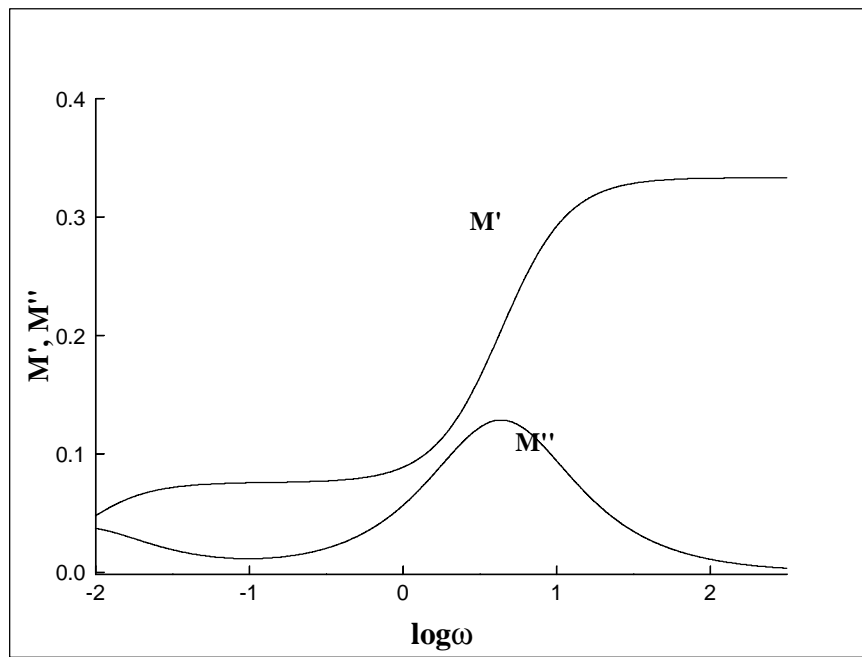


Figure 9. Schematic plots of M' and M'' -vs- $\log \omega$ for a sample represented as the equivalent circuit fig. 1(e), as derived from the data of fig. 8.

3.4. Summary of Model Circuits

In practice, various electrical equivalent circuits have been proposed for materials, but those described above are the simple building blocks that account for relaxation and conduction. An important additional feature for real materials is the blocking layer capacitance that may be present between the sample and the electrodes. This may be a permanent feature of a circuit, to be represented in the f -domain as a $[R_s, C_s]$ or $[R_p, C_p]$ element in series with the sample-circuit or may be a layer created by electrochemistry at the electrode-sample interface following application of a voltage which, as noted above, is difficult to represent using equivalent circuits whose elements have f -independent values.

In practice, it is common to represent electrode-polarization or electrode-blocking effects as a Warburg impedance that corresponds to an assembly of resistors and capacitors arranged as a fractal array [33,34]. The complex impedance takes the form

$$Z(\omega) \sim \omega^{-\beta} \quad (17)$$

where the exponent β lies between 0 and 1 and is not necessarily restricted to a value of $1/2$. It should be apparent from the above that different representations of E/D data, as $\epsilon(\omega)$, $M(\omega)$, $Y(\omega)$, $Z(\omega)$ or $\sigma(\omega)$ will emphasize, very differently, the processes of relaxation and conduction in materials. The important question arises - what information can be obtained concerning molecular processes (dipole motions, charge motions) from these individual representations? We shall see below that dipole motions are expressed conveniently as time-correlation functions that, on Fourier transformation, relate to $\epsilon(\omega)$. Charge transport processes are expressed as time-correlation functions that, on Fourier transformation, relate to $\sigma(\omega)$.

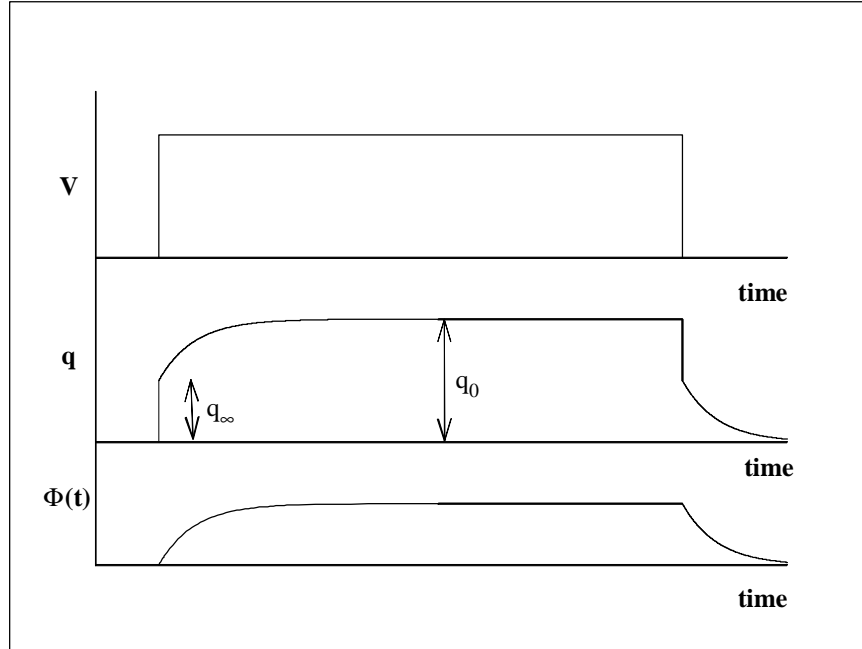


Figure 10. Schematic plots of charge $q(t)$ and normalised relaxation function $\Phi(t)$ -vs- time for a sample subjected to a step-on and step-off voltage V .

4. Distributed Circuits

For frequencies higher than $\sim 10^7$ Hz and into the microwave range, lumped circuits are replaced by distributed circuits that describe the propagation of electromagnetic waves (EM waves) through a material. As described in the major texts, especially those of Von Hippel [17, 18], the propagation coefficient $\gamma(\omega)$ is written as

$$\gamma(\omega) = \alpha(\omega) + i\beta(\omega) \quad (18)$$

$\alpha(\omega)$ is the attenuation coefficient and $\beta(\omega)$ is the phase factor for the material for $f = \omega/2\pi$

$$\beta(\omega) = 2\pi/\lambda_m = 2\pi n/\lambda_o \quad (19)$$

where λ_m and λ_o are the wavelength in the sample and in vacuum, respectively, for a given value of ω . $n(\omega)$ is a real refractive index in the expression for the complex refractive index

$$n(\omega) = n'(\omega) + in''(\omega) = n(1-ik) = \frac{i\lambda_o \gamma(\omega)}{2\pi} \quad (20)$$

We may write

$$\epsilon'(\omega) = n^2(1 - \alpha^2/\beta^2); \quad \epsilon''(\omega) = 2n^2\alpha/\beta \quad (21 \text{ a,b})$$

where we omit (ω) in α , β for convenience. Also the absorption index $k = \alpha/\beta$. In IR and UV/visible spectroscopies data are normally presented as plots of absorption (α) -vs- ω . It should be understood that this represents only one part of the behaviour, since n' will show a corresponding dispersion throughout an absorption region. The link between DRS, expressed in terms of $\epsilon(\omega)$ and quantum spectroscopies, such as IR

and UV/visible spectroscopies is obvious since they all determine the variations of $\epsilon(\omega)$ or the related $n(\omega)$ with ω through an absorption feature.

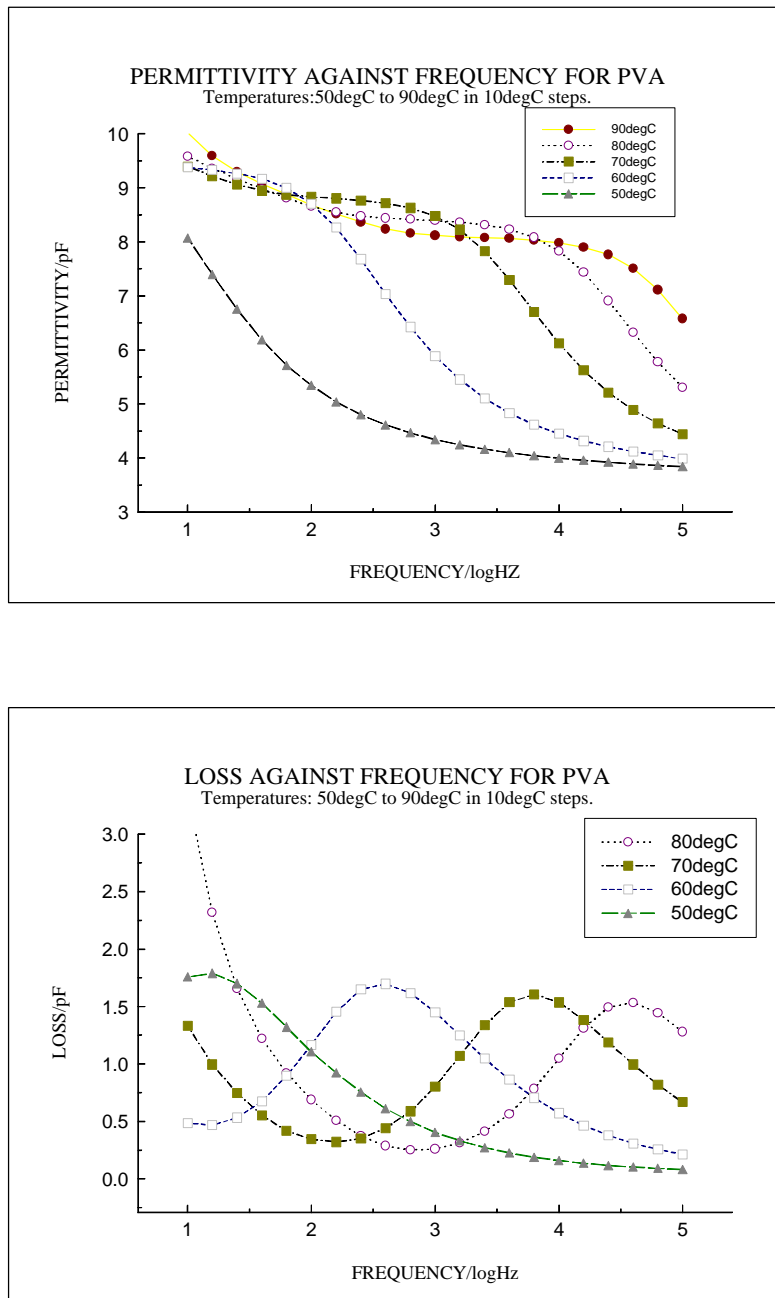


Figure 11. Plots of (a) ϵ' , (b) ϵ'' and (c) $\epsilon''/\epsilon'_{max}$ -vs- $\log(\text{frequency}/\text{Hz})$ for poly(vinyl acetate) at different temperatures showing the α -relaxation process and a conductivity tail (ref. 38).

5. PHENOMENOLOGICAL THEORIES OF RELAXATION

5.1. Single Relaxation Time Function and Distributions of Relaxation Times

The response of a linear dielectric material to a series of applied voltages may be written in terms of a super position of responses, as envisaged by Boltzmann (1874) for the analysis of mechanical creep and stress relaxation properties of solids [32, 35]. This general approach, which applies to any pattern of applied stress

(or for DRS, electric fields), is discussed in detail by Ferry [32] and by McCrum, Read and Williams [4]. For the purposes of this article, we shall be concerned initially with the response to step-on and step-off applied fields, and how the dielectric relaxation functions relate to $\epsilon(\omega)$ or the other intensive E/D quantities.

We have seen in Section 3.1 that a sample regarded as a series $[R_s, C_s]$ circuit exhibits relaxation according to the single relaxation time (SRT) equation, eqn. (8) above. In the phenomenological theory of relaxation, equivalent circuits are not assumed but a general approach is taken based on the dielectric response of a material to a step-voltage or more complication patterns of an applied voltage [1-4, 17, 18].

Fig. 10 shows the electric charge q (which is proportional to the induced electric polarization P) in a material following the step-on and step-off of an applied voltage V . The instantaneous rise and decay transients are associated with the displacement of the charge-clouds in the molecules, and this is normally described as 'electronic polarization' which is a very fast process ($t < 10^{-12}$ sec). The delayed response is due to relaxation arising from reorientation polarization due to dipoles or from interfacial polarization (Maxwell-Wagner effect)[36]. Subtracting the instantaneous components to both the rise and decay transients we obtain normalised rise and decay relaxation functions as shown in fig. 10. For a linear system

$$\Phi_r(t) = 1 - \Phi_d(t) \quad (22)$$

where subscripts r and d refer to rise and decay respectively. From the superposition relation [4] it follows that the ac response, expressed as $\epsilon(\omega)$ for a material is given by [2-4, 19, 37]

$$\epsilon(\omega) = \epsilon_\infty + (\epsilon_o - \epsilon_\infty) [1 - i\omega \mathfrak{S}(\Phi_d(t))] \quad (23)$$

where \mathfrak{S} indicates a one-sided Fourier transform. ϵ_∞ is the short-time, high frequency permittivity and ϵ_o is the long-time, low frequency permittivity. Thus DRS measurements made in the time-domain, which determine $\Phi_d(t)$, are related to DRS measurements made in the f-domain by the transform relation eqn. (23). For the model-case where $\Phi_d(t)$ is given by a single exponential function

$$\Phi_d(t) = \exp(-t/\tau) \quad (24)$$

then eqn. (23) yields the result

$$\epsilon(\omega) = \epsilon_\infty + \frac{\epsilon_o - \epsilon_\infty}{1 + i\omega\tau} \quad (25)$$

This is the familiar 'single relaxation time' equation, sometimes known as the Debye equation after Nobel Laureate Peter Debye who first used it to explain dielectric relaxation of dipolar molecules in the liquid and solid states [1-4]. Eqn. (25) is formally equivalent to eqn. (8) that was derived for a series $[R_s, C_s]$ circuit and thus gives curves for $[\epsilon', \epsilon'']$ and $[M', M'']$ as in figs. 2 and 3.. The transient current behaviour in step-off and step-on fields for that model circuit see eqns. (4) is also formally equivalent to the transient response shown in fig. 10, when it is remembered that the transient *current* is the first time-derivative of the transient *charge*.

While the SRT equation, eqn. (25) is the starting point to rationalise dielectric relaxation in polymers, liquids and liquid crystals etc. it fails to account for the shape of the dispersion and absorption curves in plots against $\log f$ for real materials. As one example, we show in fig. 11 (a) and (b) data for ϵ' and ϵ'' -vs- $\log f$ for the α -relaxation in poly(vinyl acetate) at different temperatures obtained using a Novocontrol dielectric spectrometer at Swansea[38]. The loss curves are broad and asymmetrical at each temperature of measurement, with a total half-width of ~ 1.8 units of $\log_{10}(f/\text{Hz})$ which is to be compared with 1.14 expected from the SRT equation. In order to explain such spectral-line shapes it is usual to represent $\epsilon(\omega)$ as a superposition of single relaxation-time processes having an associated distribution of relaxation times $g(\log \tau)$ say. Hence, eqn. (24) is generalized to read

$$\Phi_d(t) = \int g(\log \tau) \exp(-t/\tau) d \log \tau \quad (26)$$

and hence

$$\frac{\epsilon(\omega) - \epsilon_\infty}{\epsilon_o - \epsilon_\infty} = \int \frac{g(\log \tau)}{1 + i\omega\tau} d \log \tau \quad (27)$$

Different forms for $g(\log \tau)$ may be used to fit data, as described by Ferry [32] and by McCrum, Read and Williams [4], or $g(\log \tau)$ may be determined numerically using data for $\epsilon'(\omega)$ or $\epsilon''(\omega)$ -vs- $\log \omega$ using approximate numerical methods developed originally by Schwarzl and Staverman and their coworkers for mechanical relaxations in polymers [32]. The modern approach allows the distribution function $g(\log \tau)$ to be determined numerically by an inversion of the $\epsilon''(\omega)$ data by a procedure due to Provencher [39]. This has been illustrated recently for dielectric relaxation in polymer materials [40, 41] and a recent example is the work of Kremer published in the Novocontrol Newsletter [42].

Traditionally, it has been customary to fit plots of ϵ' and ϵ'' -vs- $\log \omega$ using empirical functions expressed in the f -domain or t -domain. The most versatile function in the f -domain is that due to Havriliak and Negami [43] which is an empirical modification of the SRT equation.

$$\frac{\epsilon(\omega) - \epsilon_\infty}{\epsilon_0 - \epsilon_\infty} = \frac{1}{(1 + (i\omega\tau)^\alpha)^\beta} \quad (28)$$

$$0 < \alpha \leq 1; 0 < \beta \leq 1$$

For $\beta=1$, the HN equation becomes the Cole-Cole equation with one 'spread' parameter α . For $\alpha=1$ the HN equation becomes the Davidson-Cole equation with one spread parameter β . Eqn. (28) generates broad, asymmetric curves for ϵ'' -vs- $\log \omega$ that are skewed to high frequencies. The HN function gives a very good representation of dielectric relaxation data in many polymers, as has been reviewed in great detail in the recent text of Havriliak and Havriliak [44].

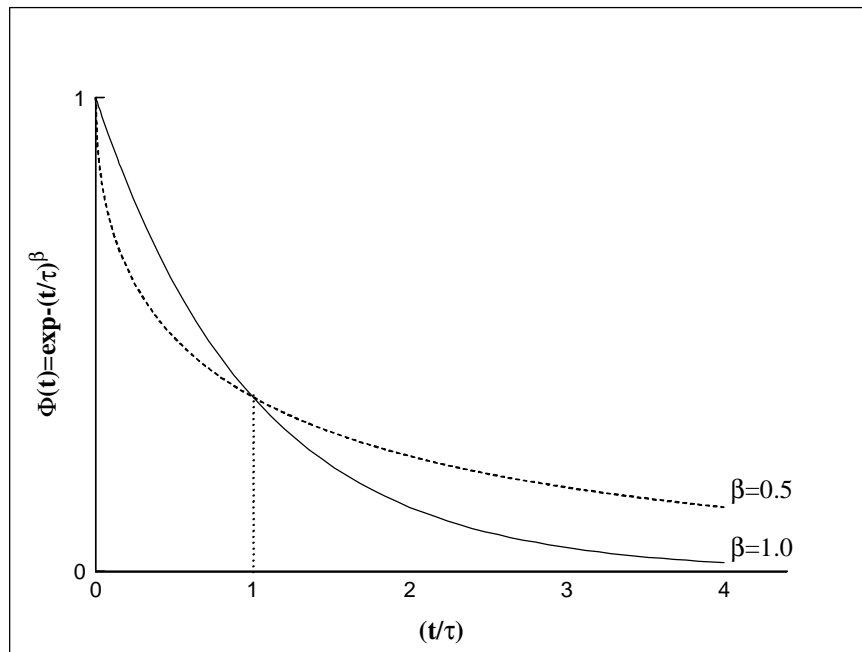


Figure 12. The decay of the relaxation function $\Phi(t/\tau)$ for a single exponential function ($\beta = 1$) and KWW stretched exponential function (for $\beta = 0.5$).

An alternative approach to broad relaxation features in the f -domain for materials is to modify $\Phi_d(t)$ without introducing a distribution of relaxation times. The stretched exponential function of Kohlrausch and later Williams and Watts is written as [45, 46]

$$\Phi_d(t) = \exp - (t/\tau)^\beta \quad (29)$$

where $0 < \beta \leq 1$. Williams and coworkers [21, 45, 46] used this empirical function to fit experimental DRS data for the α -relaxation in amorphous polymers. As one example fig. 12 shows the plot of $\Phi_d(t)$ -vs- log time for the single exponential decay function ($\beta=1$) and the KWW function, eqn. (29), for $\beta = 0.5$. The KWW function falls quickly and then for $t/\tau > 1$ decays only slowly, when compared with the single exponential decay function. This has the effect of broadening and skewing to high frequencies the curve for ϵ'' -vs- log ω derived from eqn. (23) as shown in fig. 13. Comparison with the normalized loss curves in fig. 11(c) for the α -relaxation in poly(vinyl acetate) shows that the broad asymmetric loss curves for the polymer are similar in form to those calculated from the KWW function. A good fit is obtained for $\beta = 0.56$ for poly(vinyl acetate) in this temperature range. The KWW function is used widely to fit dielectric data in the t- and f-domains for the α -relaxation in amorphous polymers [21, 24-26, 45], glass-forming liquids [47-50, 11] and ionic melts [11]. Numerical transforms of the KWW function from the t- to f-domain for the KWW equation eqn. (29) give $[\epsilon'(\omega), \epsilon''(\omega)]$ values using eqn. (23) and these have been tabulated by Koizumi and Kita [51] for β -values in the range 0.3 to 1.0. These tables complement the earlier calculations of Williams et al [45, 46] and of Moynihan et al [see ref. 46 in the paper by Moynihan [15]]. Note that Ngai and co-workers use the KWW function as a part of their coupling scheme for relaxations in polymers and complex liquids (see ref. 6, p.58 for refs. to their extensive researches).

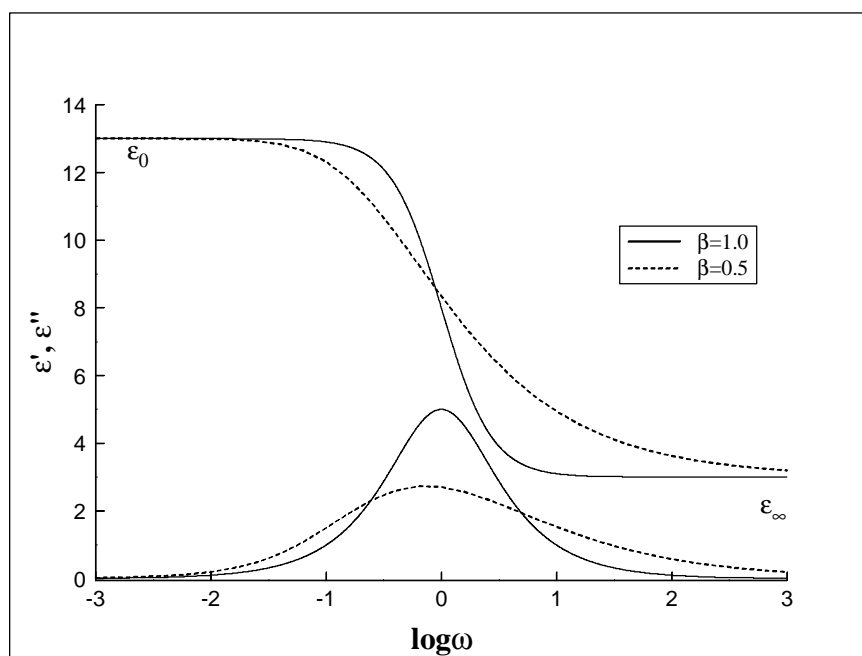


Figure 13. Schematic plots of ϵ' and ϵ'' -vs- log $\omega\tau$ for a single relaxation time function (continuous lines) and a KWW stretched exponential function with $\beta = 0.5$.

5.2. Temperature Dependence of Relaxation Times

The frequency location of the peak in ϵ'' -vs- log ω defines an average relaxation time $\langle\tau\rangle$ from $\omega_{\max}(\tau) = 1$ where $2\pi f_{\max} = \omega_{\max}$ and f_{\max} is the frequency of maximum loss. As is evident from the data of fig. 11 for the α -relaxation in poly(vinyl acetate) that $\langle\tau\rangle$ values decrease with increasing temperature. For polymers and glass-forming liquids, two dielectric relaxation processes are often observed[4, 21, 11, 50], the lower frequency α -process being associated with the microbrownian motions of molecules or chain segments within polymer chains while the higher frequency β -process is associated with local motions of whole molecules or chain-segments or side-group motions (eg for acrylate and methacrylate polymers). The temperature dependence of the α -process is usually expressed in terms of the Vogel-Fulcher equation

$$\langle\tau\rangle = A \exp [B/(T-T_{\infty})] \quad (30)$$

so the plot of $\log \langle \tau \rangle$ -vs- $(T-T_0)^{-1}$ is linear. Eqn. 30 may be rewritten as the Williams-Landel-Ferry equation.

$$\ln \langle \tau_1 \rangle / \langle \tau_2 \rangle = \frac{C_1(T_1 - T_2)}{C_2 + (T_1 - T_2)} \quad (31)$$

where C_1 and C_2 are material constants and $\langle \tau_1 \rangle$ and $\langle \tau_2 \rangle$ are the values at T_1 and T_2 respectively. The β -process usually conforms to the Arrhenius equation

$$\langle \tau \rangle = C \exp (H/RT) \quad (32)$$

where H is an apparent activation energy and R is the gas constant. In this case, the plot of $\log (\tau)$ -vs- T^{-1} is linear, yielding a value for H . Recently, there has been much discussion of the use of the VF equation and alternative equations have been proposed (52).

It is usually accepted that eqn. 30 can be derived on the assumption that $\langle \tau \rangle$ is related to a time-averaged quantity called the 'free volume' [32]. However, that concept is difficult to reconcile with the observation that constant volume apparent activation energies, H_v say, are ~ 0.8 of the constant pressure activation energies, H_p say. This difficulty has been discussed in some detail [26].

There is a limited literature on the effects of applied pressure on $\langle \tau \rangle$ for polymers [21]. Increase in pressure leads to a marked increase in $\langle \tau \rangle$ for α -processes, with $(\partial \log \langle \tau \rangle / \partial P)_T$ being in the range 1-3 kbar⁻¹. The effect of pressure on β -processes is smaller with $(\partial \ln \langle \tau \rangle / \partial P)_T$ being in the range 0.1 - 0.5 kbar⁻¹. Overlapping processes are conveniently separated using pressure as a variable, as is illustrated by the splitting of an $\alpha\beta$ process into α and β processes in amorphous polymers [21].

Finally, we note that the Adam-Gibbs equation [53, 35] is often used to express $\langle \tau(T) \rangle$ for the α -relaxation in polymers and glass-forming liquids [35].

$$\langle \tau(T) \rangle = E \exp \frac{F}{TS_c(T)} \quad (33)$$

where E and F are material constants and $S_c(T)$ is the configurational entropy of the material. As $S_c(T)$ decreases with decreasing temperature $\langle \tau(T) \rangle$ increases correspondingly. This equation is used extensively by Matsuoka [35] for different relaxation phenomena in polymers and has the feature that if $S_c \rightarrow 0$ then $\langle \tau \rangle \rightarrow \infty$ at a finite temperature - which is to be compared with the behaviour of the VF equation, eqn. (30) for $T \rightarrow T_\infty$.

6. MOLECULAR THEORIES OF RELAXATION

6.1 The Time-Correlation Function Approach to Dielectric Relaxation.

In the early theories of dielectric relaxation of dipolar liquids and solids, an equation for the rotational motions of the dipoles was assumed and was solved in the presence of a.c. or step electric fields [1,2]. Such theories were extremely complicated to elucidate and gave little physical insight into the nature of molecular motions that give rise to the dielectric behaviour of a material. A considerable advance was made by Glarum [54] and by Cole [55] who used the linear response theory of Kubo and others to relate $\epsilon(\omega)$ to field-free molecular time-correlation functions (TCF) for the reorientational motions of the dipolar molecules, independent of any particular mechanism for the tumbling process. Their approach for small molecules in liquids and solids was extended by Cook, Watts and Williams [56] to the case of polymer chains in the liquid and amorphous solid states. The TCF approach to dielectric relaxation has been reviewed by Williams [19, 21, 23, 25, 26, 28, 37]. Despite the fact that some of these papers are nearly 30 years old, the TCF approach to dielectric relaxation is still not widely-used, largely due to the non-familiarity of scientists with time-dependent statistical mechanics. In order to familiarize the reader, we explain the essential aspects of TCF for dielectric relaxations in a liquid or amorphous polymer composed of dipolar molecules.

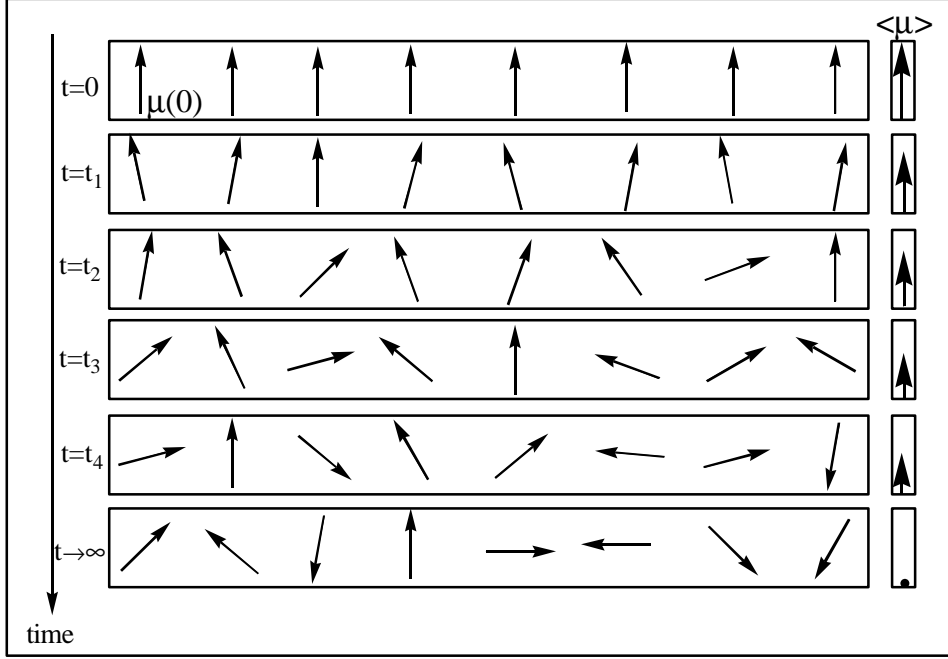


Figure 14. Illustration of the randomisation, with time, of a sub-ensemble of dipole vectors in a liquid that all have the same dipole orientation at $t = 0$. As time develops microbrownian motions move the dipoles away from their initial orientation so the average dipole moment per molecule $\langle \mu \rangle$ taken over the sub-ensemble decreases steadily from $\mu(0)$ to zero with increasing time. This loss of orientation correlation with time is the basis of the vector-vector time correlation function $\Phi(t)$ for dielectric relaxation in liquids and amorphous solids (e.g. amorphous polymers).

Consider a macroscopic volume V in a material to contain N molecules each having a dipole moment μ (a vector quantity) whose direction changes with time due to the natural thermal motions within the material. At $t = 0$ identify all those molecules that have the same orientation, as a subset N_1 of N . Fig. 14 shows these N_1 dipoles at $t = 0$. As time evolves, molecular motions move the dipole orientations away from $\mu(0)$, as indicated in the figure, so as $t \rightarrow \infty$ they have, on average, no correlation with the original orientation. The average projection per molecule at time t on the original direction at time zero is $\langle \cos \theta(t) \rangle = \mu(0) \cdot \mu(t) / \mu(0) \cdot \mu(0)$ which decreases with increasing time from $\langle \cos \theta(t) \rangle = 1$ at $t = 0$ down to zero for $t \rightarrow \infty$. The dipole moment TCF is equal to the further average of $\langle \cos \theta(t) \rangle$ taken over all initial orientations of the dipole at $t = 0$, and over all other molecules in the ensemble of N molecules. In normalized form the TCF is written as $\Phi_{\mu}(t)$. For this case of an amorphous system, since all initial directions of dipoles are equally probable and all molecules are equivalent it follows that

$$\Phi_{\mu}(t) = \frac{\mu(0) \cdot \langle \mu(t) \rangle}{\mu^2} = \frac{\langle \mu(0) \cdot \mu(t) \rangle}{\mu^2} \quad (34)$$

According to linear-response theory [2,3,19,37]

$$\frac{\epsilon(\omega) - \epsilon_{\infty}}{\epsilon_0 - \epsilon_{\infty}} \cdot p(\omega) = 1 - i\omega \Im[\Phi_{\mu}(t)] \quad (35)$$

where $p(\omega)$ is an internal field factor [39, 37] and \Im indicates a one-sided Fourier transform. Thus, if we know how the dipole moment correlation function $\Phi_{\mu}(t)$ decays to zero with time then eqn. (35) can be used to obtain $\epsilon(\omega)$. For small-step rotational diffusion of molecules we have [37]

$$\Phi_{\mu}(t) = \exp - 2 D_r t \quad (36)$$

i.e. an exponential decay with $\tau_{\mu} = (2D_r)^{-1}$ and where D_r is the rotational diffusion coefficient. Setting $p(\omega) = 1$ then eqn. (35) and eqn.(36) yield the single relaxation time equation, of the same form as eqn. (8) only τ_{μ} replaces τ_{RC} . Hence curves of $[\epsilon', \epsilon'']$ -vs- log frequency will take the form of fig. 2. Thus simple rotational diffusion of dipoles gives dielectric relaxation in the f-domain as a single relaxation time process and the interpretation of such behaviour is understood physically in terms of $\Phi_{\mu}(t)$.

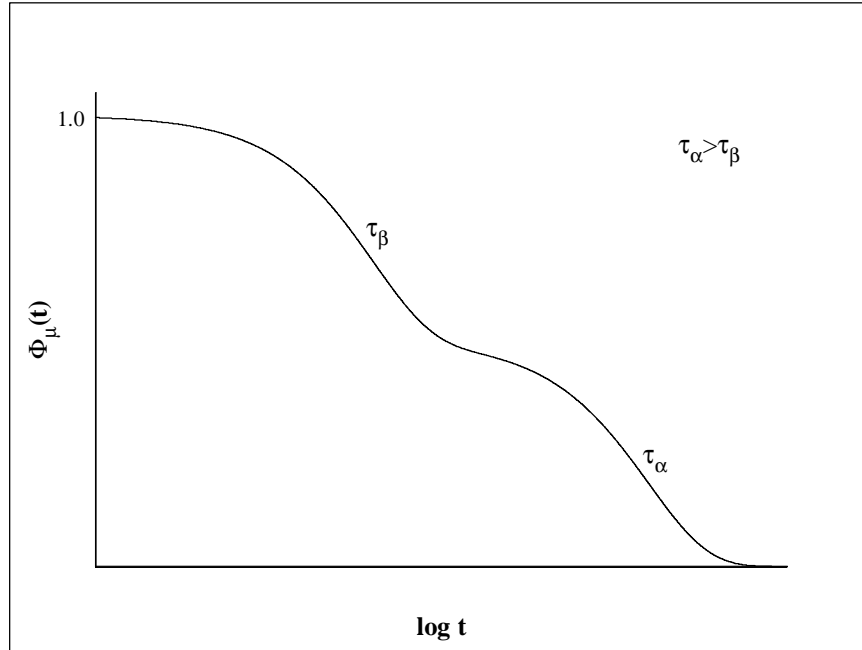


Figure 15(a). Schematic illustration of the decay of the dipole moment correlation function $\Phi_{\mu}(t)$ with time in two stages; by a fast β -process and a slower α -process.

Suppose that in a liquid on an amorphous solid that at short times local molecular motions lead to a partial net reorientation of the dipole vectors and hence to a partial decay in $\Phi_{\mu}(t)$ as shown schematically in fig. 15(a). At longer times microbrownian motions of molecules fully randomize the dipole orientations and $\Phi_{\mu}(t)$ falls to zero, as shown in the figure. Application of eqn. (35) leads to two relaxation processes in the frequency domain as shown in fig. 15(b). The short-time β -process transforms to give the high-frequency β -process, the long-time α -process gives the low-frequency α -process. Such multiple relaxations occur in glass-forming liquids and amorphous polymers [4, 11, 21-32, see especially ref. 29].

The dielectric behaviour arising from different motional processes for the dipoles can be obtained by first determining the form of $\Phi_{\mu}(t)$ for the particular process and then using eqn. (35) to deduce $\epsilon(\omega)$. The following models can be elucidated in this way :- Rotational diffusion by intermediate or large-angle jumps; collision-interrupted rotational motions; barrier-hopping in site-systems of different symmetries; internal motions of molecules [19, 37] and relaxation involving chemical relaxation between species [57]. If the motions are simulated by computer, then $\Phi_{\mu}(t)$ may be obtained numerically for insertion into eqn. (35). Thus, the TCF approach to dielectric relaxation of dipoles in liquids and solids requires $\Phi_{\mu}(t)$ to be known analytically or numerically and this allows $\epsilon(\omega)$ to be determined. The TCF approach is also used for liquid crystals and liquid crystal polymers [58-60]. In these cases there are, for nematic liquid crystals, two principal permittivities $\epsilon_{||}(\omega)$ and $\epsilon_{\perp}(\omega)$ measured parallel and perpendicular, respectively, to the liquid crystal director axis n . [58-60]. The details of the derivations are too complex to be given here but it can be shown that $\epsilon_{||}(\omega)$ is related to two correlation functions $\Phi_{\mu_{00}}(t)$ and $\Phi_{\mu_{01}}(t)$ and $\epsilon_{\perp}(\omega)$ similarly to further functions $\Phi_{\mu_{10}}(t)$

and $\Phi_{\mu_{11}}(t)$ [59] where these functions relate to the motions of $\mu_{||}$ and μ_{\perp} (longitudinal and transverse component dipole moments) of the molecules in the anisotropic potential of the liquid-crystalline state. Thus DRS measurements probe the anisotropic motions of the liquid crystalline groups as revealed in the four relaxation modes $\Phi_{\mu_{ij}}(t)$ indicated above.

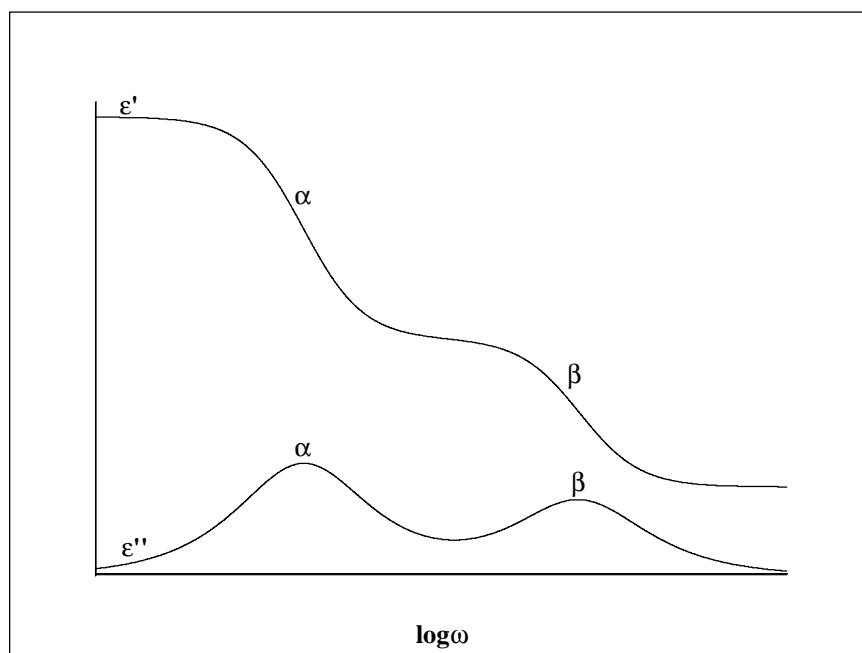


Figure 15(b). Schematic plots of ϵ' and ϵ'' -vs- $\log \omega$ corresponding to the two-stage decay function shown in fig. 15(a).

6.2. Applications of the TCF Approach

The theoretical basis of TCFs as they apply to dielectric relaxation, fluorescence depolarization, nuclear magnetic resonance relaxation, quasi-elastic light scattering and neutron scattering and band-shapes in infrared and Raman spectroscopies has been reviewed, see e.g. refs.19, 37 and 61. The TCF theory for dielectric relaxation in polymers was first given by Cook, Watts and Williams [56] and was reviewed by Riande and Daiz [62]. The TCF theory for dielectric relaxation in barrier models possessing different symmetries was given by Williams and Cook [63] and is applicable to rotator-phase molecular crystals [64]. The nature of α , β , $\alpha\beta$ relaxations in amorphous polymers was rationalized by Williams and coworkers using a TCF approach to partial and total relaxations (see e.g. refs. 21-23, 25-29 for reviews, especially ref. 29 for the most recent account). Long-range motions of polymer chains having a cumulative dipole moment, as in polypropylene oxide and polyisobutylenes, give rise to dielectric relaxation, as demonstrated by Stockmayer and Baur [65] and Adachi and coworkers [66, 67]. The TCF for dielectric relaxation in such polymers including local motions and long-range motions was given by Adachi [66, 67] (see also Schönhal's [68] for a recent review). The TCF theory for dielectric relaxation in liquid crystals and liquid crystal polymers has been given by Attard [69] and Araki and coworkers [59], revealing anisotropy of $\epsilon(\omega)$ and relaxation arising from four active dielectric relaxation modes. Williams [70] showed how dielectric relaxation could arise for systems undergoing chemical relaxation, eg $A = B$ and $A + B = C$. This theory was applied recently to dielectric relaxation in thermoreversible polymer networks [71].

It is apparent from these works that if a particular model is proposed for dielectric relaxation in a material, then the favoured procedure for elucidating $\epsilon(\omega)$ is to form the dipole moment TCF and use eqn. (35), thus avoiding solving equations of motion in the presence of a perturbing electric field.

6.3. $\epsilon(\omega)$ and Alternative Representations of Relaxation Data

It is evident that in the case of dielectric relaxation arising from motions of dipoles that experimental data should be presented as $\epsilon(\omega)$ since it is this quantity that relates directly to the molecular property $\Phi_{\mu}(t)$ (see eqn. (35)). In such cases, $M(\omega)$, $Z(\omega)$ and $\sigma(\omega)$ are inappropriate forms since no simple direct relationship exists between those quantities and the TCF, $\Phi_{\mu}(t)$. Consider $M(\omega)$. We have seen in eqns. (8) and (10) that a SRT process in $\epsilon(\omega)$ converts formally into a SRT process in $M(\omega)$. Thus, one might suppose that either form would be equally informative about the underlying molecular processes. However, $\epsilon(\omega)$ will relate to τ_{ϵ} which will be closely related to τ_{μ} (see eqns. (35)) whereas $\tau_M = (\epsilon_{\infty}/\epsilon_0)\tau_{\epsilon} = (M_0/M_{\infty})\tau_{\epsilon}$. Thus, τ_M relates not only to the molecular quantity τ_{μ} but to the quantities ϵ_{∞} and ϵ_0 which have no relation to the dynamical properties of a material. Therefore dipole relaxation behaviour is best expressed using $\epsilon(\omega)$ and not $M(\omega)$. In practice, ionic conduction losses can obscure the loss arising from dipole relaxation and conversion to $M''(\omega)$ will diminish the conduction contribution. If ϵ_0 and ϵ_{∞} are known then τ_{μ} can be calculated from τ_M . We shall discuss below the information obtainable from $M(\omega)$ and $\sigma(\omega)$ for systems exhibiting ionic conduction.

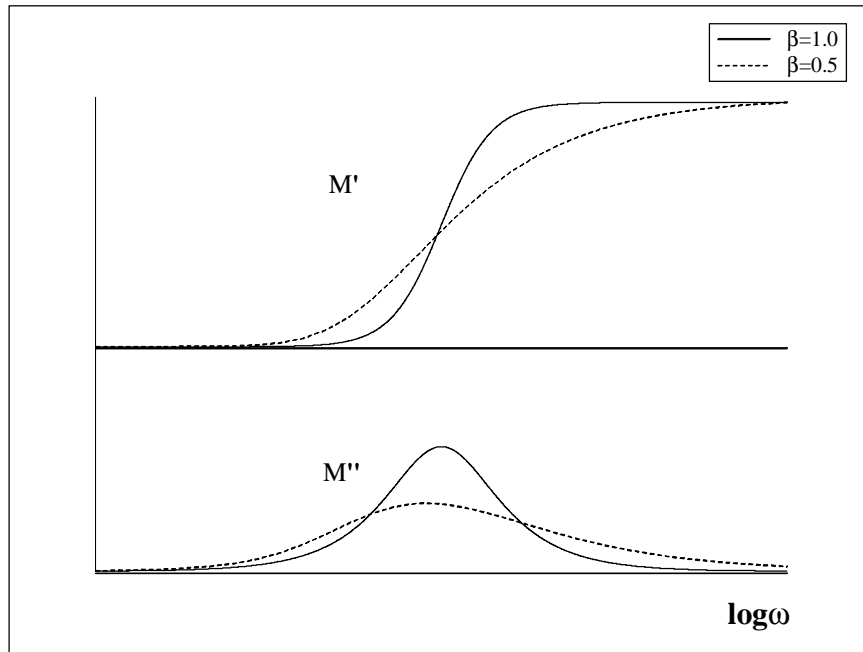


Figure 16. Comparison of plots of (M' , M'') -vs- $\log \omega$ for a single relaxation time function ($\beta = 1$) and a KWW function with $\beta = 0.5$.

7. PHENOMENOLOGICAL THEORIES OF CONDUCTION

7.1. Single relaxation time function and distributions of relaxation times

In Section 3.2., it was shown that $Z(\omega)$ and $M(\omega)$ exhibited relaxation behaviour for the parallel $[R_p, C_p]$ circuit despite the fact that this circuit does not exhibit transient (relaxation) behaviour in response to a step-applied field. Phenomenological theories of conduction need not use electrical equivalent circuits explicitly. Electrical relaxation in ionic solids and liquids is attributed to the motions of ions and a description of the electrical properties may be given in terms of electric-field relaxation, as described by Moynihan and coworkers [12 - 15] who write

$$M(\omega) = M_{\infty}(1 - \Im[-d\phi(t)/dt]) = M_{\infty}i\omega \Im[\phi(t)] \quad (37)$$

where \Im is a one-sided Fourier transform and $\phi(t)$ is the normalised relaxation function $E(t)/E(0)$ for the relaxation of the electric field in a sample under the constraint of a constant dielectric displacement. As emphasized by Nowick et al [72] if there were no dependence on the real permittivity ϵ' and real conductivity

σ' on frequency for a material then $M(\omega)$ would be given by the single relaxation time equation and $M''(\omega)$ would be a single 'Debye' peak with $\tau_{RC} = R_p C_p$ as we have seen for the parallel $[R_p, C_p]$ circuit described in Section 3.2 (see eqn. (15)). This corresponds to $\phi(t)$ in eqn. (37) being given by a single exponential decay function

$$\phi(t) = \exp - t/\tau_M \quad (38)$$

which on insertion into eqn. (37) gives eqn. (15) with $\tau_M = R_p C_p$.

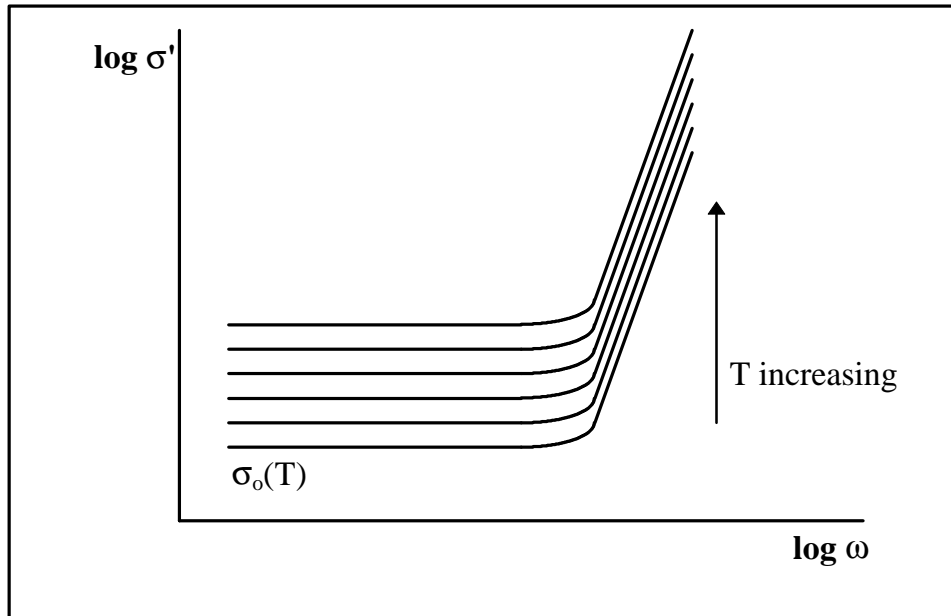


Figure 17. Schematic plots of $\log \sigma'$ -vs- $\log \omega$ for a system exhibiting ionic conduction.

Moynihan and coworkers [12-15] found that a good description of the electrical relaxation behaviour of ionic solids and liquids was obtained using eqn. (37) together with a KWW function (eqn. 29) for $\phi(t)$. As shown schematically in fig. 16 the plots of $M'(\omega)$ and $M''(\omega)$ broaden and become asymmetric when $\beta < 1$. Examples of recent experimental data that show such behaviour in $M(\omega)$ are 0.4 $\text{Ca}(\text{NO}_3)_2$ -0.6 KNO_3 (CKN) melt [13], 33% LiCl in glycerol [13] and $\text{Na}_2\text{O} \cdot 0.3\text{SiO}_2$ glass [72]. Extensive conduction data are reported for these ionic solids and many other systems in refs. 30 and 31. One example of master curves of M' and M'' -vs- $\log \omega$ for a CdF_2 - LiF - ARF_3 - PbF_2 glass is shown by Hasz, Moynihan and Tick [13] which are well-fitted with $\beta = 0.77$. The same approach has been found to give an excellent representation of $M(\omega)$ data for a wide range of ionic materials, including electrolytes and polymer-electrolytes. According to Moynihan [15] and Greaves and Ngai [73] the dc conductivity is given by

$$\sigma_o = \epsilon_v \beta / M_\infty \Gamma(1/\beta) \quad (39)$$

where Γ indicates the gamma function. Thus, this approach represents the electrical behaviour of an ionically-conducting material in terms of $M(\omega)$ and $\phi(t)$. The KWW behaviour observed experimentally is considered to arise from a distribution of processes having different τ_M values, analogous with eqn. (26) above. As alternatives to the KWW function the Davidson-Cole empirical function, Cole-Cole or HN functions may also be used to represent $\phi(t)$ (see Moynihan [15]).

As we have discussed earlier, the alternative representations of data as $\epsilon(\omega)$, $Y(\omega)$, $Z(\omega)$ and $\sigma(\omega)$ may be used for the electrical properties of ionically-conducting systems. Experimental data for the real conductivity $\sigma'(\omega)$ of amorphous materials follow that shown schematically in fig. 17 (see refs. 30 and 31 for numerous examples). At low frequencies, $\sigma'(\omega)$ is a constant at the d.c. value $\sigma_o(T)$. As temperature T is increased the values of $\sigma_o(T)$ increase. For a fixed temperature, $\sigma'(T)$ increases at high frequencies according to a power law

$\sigma'(\omega) \sim \omega^p$, where $0 < p \leq 1$ and p increases towards unity as T increases. It is usual to express $\sigma'(\omega, T)$ as the empirical relation [74, 72, 15]

$$\sigma'(\omega) = \sigma'_{dc} + A\omega^p \quad (40)$$

Moynihan [15] has shown how broad relaxation functions used in $M(\omega)$ in eqn. (37) lead to calculated curves for $\sigma'(\omega)$ that have constant values σ_0 at low frequencies and power-law behaviour at high frequencies. The exponent in $\sigma'(\omega) \sim \omega^p$ is approximately equal to $(1 - \beta)$ and $(1 - \gamma)$ for the KWW and Davidson-Cole relaxation functions, respectively [15], where β and γ are the respective spread parameters.

Moynihan [15] has given an excellent review of the analysis of electrical relaxation in ionic materials. He shows the appearance of $M(\omega)$, $\sigma(\omega)$ and the complex resistivity $\rho(\omega)$ for representative systems and how they may be analysed using the E-field relaxation function $\phi(t)$ and, further, how the KWW, Davidson-Cole functions and eqn. (40) may be used consistently to fit the experimental data. The origins of the non-exponential forms for $\phi(t)$ that are used to fit data for ionic materials, such as $\text{Li}_2\text{O} - \text{Al}_2\text{O}_3 - 2\text{SiO}_2$ glass, are not explained in this phenomenological theory. The fact that such non-exponential time-functions (eg the KWW stretched exponential function) can be expressed as the Hilbert transform of a distribution of relaxation times (as in eqn. (26)) does not give any physical significance to that distribution. One might consider the generalization of the model $[R_p, C_p]$ circuit (Section 3.2) to include an assembly of such elements, all in parallel but of different $[R_p, C_p]$ values, to try to generate a distribution in $\phi(t)$. However, such an assembly is formally equivalent to a single $[R'_p, C'_p]$ circuit so will have only a single time constant $R'_p C'_p$.

In common with the behaviour described in Section 5.2, the electric-field relaxation times for ionic materials also depend on temperature in accord with the Vogel-Fulcher or Arrhenius equations. A description of the behaviour of different materials is beyond the scope of this article, but many examples are shown in refs. 30 and 31.

8. MOLECULAR THEORIES OF IONIC CONDUCTION

The random motions of ions in liquids and amorphous solids in the absence of an applied field are conveniently described using the time-dependent diffusion coefficient $D(t)$ defined by the Einstein relation [75]

$$D(t) = \langle r^2(t) \rangle / 2dt \quad (41)$$

where $\langle r^2(t) \rangle$ is the mean squared displacement of an ion at time t with respect to its position at $t = 0$. d is the Euclidean dimension of the system ($=3$ for a liquid or amorphous solid). The complex electrical conductivity $\sigma(\omega)$ for ion-motions is related to $D(t)$ by the Nernst-Einstein relation.

$$\sigma(\omega) = D(\omega) p e^2 / kT \quad (42)$$

where e and k have their usual significance and p is a scaling factor [75]

$$D(\omega) = -\omega^{-2} \lim_{\delta \rightarrow 0} \int_0^{\infty} \langle r^2(t) \rangle \exp(i\omega t - \delta t) dt \quad (43)$$

From eqns. (41-43) we see that $\sigma(\omega)$ is related, by a Fourier-Laplace transform, to the mean-squared displacement of the ions with time. A full treatment needs to include the diffusion of both ions, each with their own diffusion coefficient $D(t)$.

For the special case where $\langle r^2(t) \rangle / t$ is independent of time, D is a constant and insertion of eqn. (41) into eqns. (42) and (43) gives $\sigma'(\omega)$ as a constant, independent of frequency. As indicated above, practical systems behave as shown in fig. 17 with $\sigma'(\omega)$ increasing with increasing frequency at high frequencies. Thus an explanation for this experimental behaviour is that $D(t)$ depends strongly upon time, giving, at long times, apparent normal diffusion with constant D (and hence constant $\sigma'(\omega)$ at low frequencies) and more complicated behaviour at short times. It is difficult to derive $D(t)$ analytically for models for ion motion but considerable progress has been made by numerical simulations for hopping motions of ions. As one example we quote the work of Funke [76] who has simulated the hopping motions of ions in a periodic lattice potential

and a cage-effect potential due to Coulombic interactions. They show the following. As indicated schematically in fig. 18, at short-times (regime I) the averaging of the ion-motions is over individual hops of individual ions and in this range $\langle r^2(t) \rangle$ increases linearly with time. At intermediate times (regime II) correlations between forward and backward hops, conditioned in the model leads to a lowering of the slope of the plot of $\langle r^2(t) \rangle$ -vs- time and gives, in the simulation of Funke, the power law relation $\langle r^2(t) \rangle \propto t^p$. At longer times (regime III) only successful hops contribute to $\langle r^2(t) \rangle$ so the Einstein relation $\langle r^2(t) \rangle \propto t$ is obeyed in this range. Funke used eqns. (41) - (43) to calculate $\sigma'(\omega)$, which was found to take the form shown in fig. 19. Therefore the experimental data (shown schematically in fig. 17) are reproduced qualitatively by this theoretical model and motions in regimes II and III now have a physical interpretation. Regime I occurs at high microwave frequencies ($>10^{11}$ Hz) and has yet to be documented sufficiently for a range of systems in order to check experimental data with this theoretical model. We note that Funke [76] has compared the results of his jump-diffusion model to those of Ngai based on the KWW equation (see ref. 76 for details). It is evident that a number of other models for the translational motions of ions could give rise to Einsteinian diffusion at long times (regime III) and power-law behaviour at shorter times (regime II).

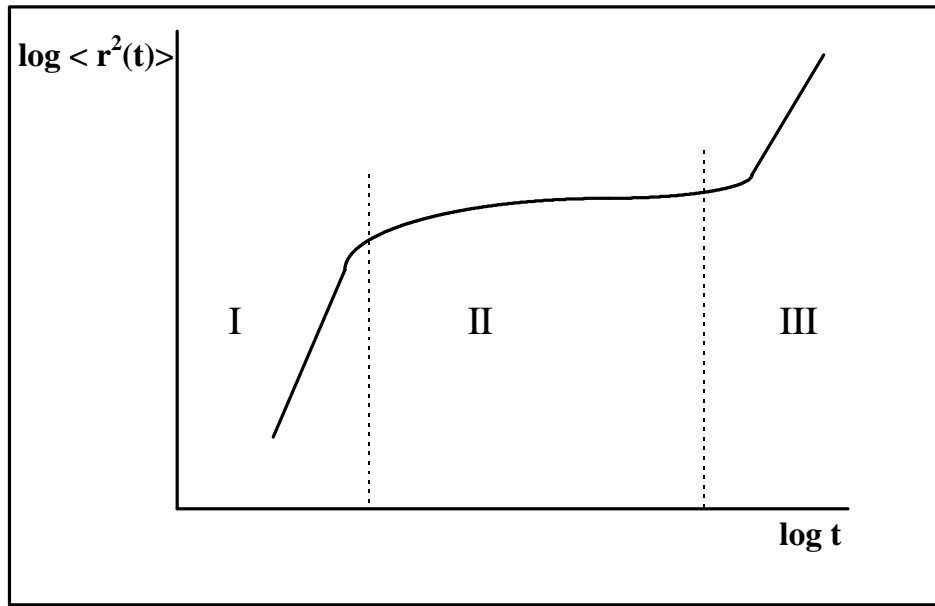


Figure 18. Plot of $\log \langle r^2(t) \rangle$ -vs- \log time for a model system exhibiting ionic conduction, showing different behaviour in regions I, II and III. After Funke [76] (see text).

An alternative approach to eqns. (41) - (43) that connect $\sigma(\omega)$ to $\langle r^2(t) \rangle$ is that involving the velocity autocorrelation function for ion motions. Forsyth et al. write [77].

$$\sigma(\omega) = \frac{1}{3kT.V} \int_0^{\infty} \langle j(0).j(t) \rangle \exp i\omega t \, dt \quad (44)$$

Where $\langle j(0).j(t) \rangle$ is the current-current time-correlation function for ion-motions.

$$j(t) = \sum q_i v_i \quad (45)$$

where q_i and v_i are charge and velocity of ion i , the sum is taken over all ions in the volume V . For a singly-charged species, $\langle j(0).j(t) \rangle$ is related to the velocity-velocity time-correlation function $\langle v(0).v(t) \rangle$ for the ensemble by

$$v(0).v(t) \rangle = q^2 \langle j(0).j(t) \rangle \quad (46)$$

Note that the current TCF and velocity TCF both include cross correlation terms between ions. For a single ion, the diffusion coefficient D is defined as

$$D = \frac{1}{3} \int_0^{\infty} \langle v(0).v(t) \rangle dt \quad (47)$$

So D is a time-averaged quantity (a transport coefficient). For Einsteinian diffusion we see that

$$D = \langle r^2(t) \rangle / 6t = \frac{1}{3} \int_0^{\infty} \langle v(0) \cdot v(t) \rangle dt \quad (48)$$

Using a molecular dynamics simulation procedure, Forsyth et al [77] have calculated $\langle r^2(t) \rangle$ -vs- time for a model of an ionic mixture (concentrated NaCl solutions in H_2O).

Thus eqns. (42) with (43) and eqn. (44) relate $\sigma(\omega)$ in different ways to the diffusional motions of ions in a liquid or solid amorphous material. Note that the total velocity correlation function for the ions could be determined from data presented as $\sigma(\omega)$ -vs- $\log \omega$ by Fourier inversion of eqn. (44).

It is apparent from the above that experimental electrical data for conducting systems including polymer electrolytes [see Meyer, ref. 78 for a recent review] may be conveniently expressed as plots of $M(\omega)$ and $\sigma(\omega)$ -vs- $\log \omega$, and that phenomenological theory is well-established for both representations. It is clear that molecular interpretations of $\sigma(\omega)$ exist in terms of the motions of ions as expressed by $\langle r^2(t) \rangle$, $\langle v(0) \cdot v(t) \rangle$ and $D(t)$. It is not apparent how $\phi(t)$, which occurs in $M(\omega)$, may be related simply to these dynamic molecular quantities since there is a reciprocal relation between $M(\omega)$ and $\sigma(\omega)$ (see eqn. (6) above).

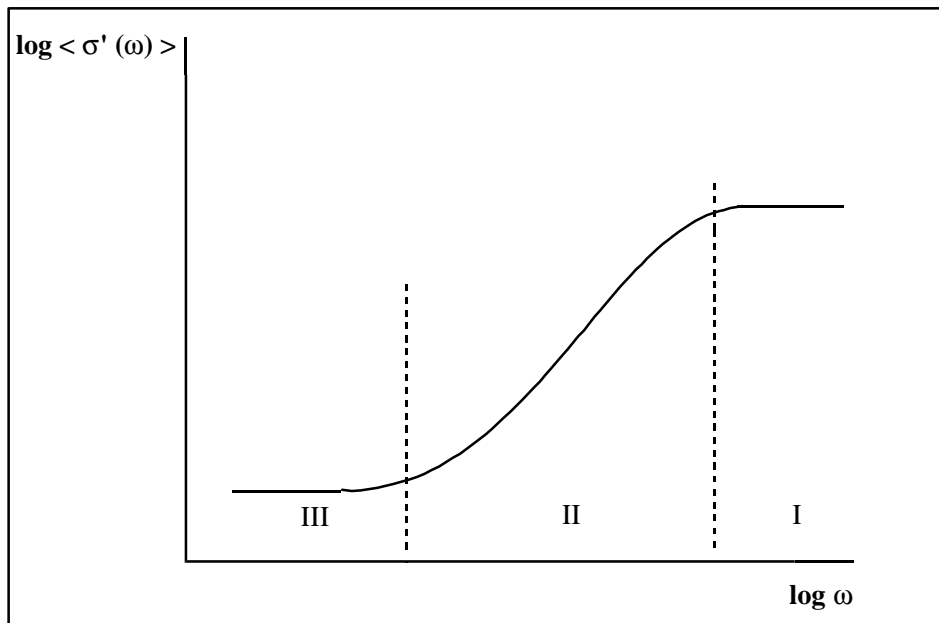


Figure 19. Plot of $\log \sigma'(\omega)$ -vs- $\log \omega$ for the model system exhibiting ionic conduction (fig. 18). After Funke [76] (see text).

9. SUMMARY

The electrical/dielectric properties of materials can be presented in different ways, as the intensive quantities of permittivity, electrical modulus, conductivity and resistivity, which emphasise differently the polarization and conduction behaviour of a material. The measured quantities $Y(\omega)$, $Z(\omega)$ may be re-expressed in terms of these intensive electrical/dielectric quantities, using equivalent lumped circuit theory. It is shown how model circuits lead to classical relaxation and conduction behaviour in the frequency domain. Phenomenological descriptions of relaxation and conduction have been described and it is shown (i) how $M(\omega)$, $\sigma(\omega)$ are related to time-dependent relaxation functions and (ii) how empirical relaxation functions may be used to represent electrical/dielectric behaviour in the t- and f-domains. Molecular theories of the electrical/dielectric properties of systems exhibiting relaxation and conduction have been outlined briefly. It is shown that the reorientational motions of dipolar molecules are conveniently expressed in terms of the dipole moment correlation function $\Phi_{\mu}(t)$ and that $\epsilon(\omega)$ is obtained via the Fourier transform of this time-function. The translational motions of ionic species that lead to electrical conduction in a material are conveniently expressed in terms of the mean squared displacement or the velocity correlation function of the ions and $\sigma(\omega)$ is obtained via the Fourier transform of these time functions. Thus dielectric relaxation due to dipole motions and f-dependent conduction due to ion-motions in materials are understood in terms of molecular properties and the dynamics of molecules and ions.

This account has attempted to make clear the essential theories that underpin the electrical/dielectric properties of materials. It has only summarized the different phenomenological and molecular theories, but sufficient references have been given where the detailed derivations and mathematical analyses are described.

This article should help to answer the following questions:

- How should experimental data be presented ($\epsilon(\omega)$, $M(\omega)$, $\sigma(\omega)$) for molecular materials exhibiting (i) relaxation and (ii) conduction behaviour?
- How do the observed properties ($\epsilon(\omega)$, $M(\omega)$, $\sigma(\omega)$) relate to molecular properties such as dipole moment, ionic-charge, dynamics of rotational and translational motions of species for each system?

A number of aspects of relaxation and conduction have not been considered here. The relaxation strength $\Delta\epsilon = \epsilon_0 - \epsilon_{\infty}$ for dipolar relaxation behaviour is an equilibrium property of a system. $\Delta\epsilon$ is proportional to the concentration of dipole species and to the mean-squared dipole moment $\langle\mu^2\rangle$ per molecules [1-4]. Thus $\Delta\epsilon$ depends on chemical structure and molecule-conformation as has been explained [1-4].

Owing to the introductory nature of this article, we have not described the coupling-scheme of Ngai and coworkers [79] that is based on the KWW function or the mode-mode coupling approach of Götze and coworkers [80, 81] which is based on a memory-function formalism. Both approaches are widely-applied to dielectric and electrical-conductivity relaxations in polymers and glass-forming liquids. Williams [28, 82] has given a critical account of the application of mode-mode coupling theory to dielectric α -relaxations in polymers and glass-forming liquids.

Finally, we note the increasing interest in the use of microwaves in inorganic and organic synthesis, where reactions are conveniently carried out in shorter times and with possibly different mechanisms when compared with the normal thermal-preparation conditions. This subject has been reviewed [83, 84] and it appears that theoretical treatments of reactions in the presence of the heating generated by microwave dielectric losses will be of some interest in the future.

10. ACKNOWLEDGEMENTS

The authors wish to thank Professor G.R. Davies of Leeds University for drawing ref. 77 to their attention. The EPSRC is thanked for the award of a studentship to D.K.T.

References

1. C P Smyth, *Dielectric Behaviour and Structure*, McGraw-Hill, New York, 1955.
2. N Hill, W E Vaughan, A H Price and M Davies, *Dielectric Properties and Molecular Behaviour*, Van Nostrand, New York, 1969.
3. C J F Böttcher and P Bordewijk, *Theory of Electric Polarization*, 2nd Ed., Vol. 2, Elsevier, Amsterdam, 1978.
4. N G McCrum, B E Read and G Williams, *Anelastic and Dielectric Effects in Polymeric Solids*, Wiley, London 1967 and Dover Publ., New York, 1991.
5. A R Blythe, *Electrical Properties of Polymers*, Cambridge University Press, Cambridge, 1979.
6. J P Runt and J J Fitzgerald, *Dielectric Spectroscopy of Polymeric Materials*, ACS Publications, Washington DC, 1997.
7. A S Nowick and B S Berry, *Anelastic Relaxation in Crystalline Solids*, Academic Press, New York, 1972.
8. A R West, J T S Irvine and D C Sinclair, *Advanced Mater.*, 1990, **2**, 133.
9. A R West, D C Sinclair and N Hirose, *J. Electroceramics*, 1997, **1**, 65.
10. A R West, *J. Mater. Chem.*, 1991, **2**, 157.
11. J Wong and C A Angell, *Glass, Structure by Spectroscopy*, Marcel Dekker, New York, 1976.
12. P B Macedo, C T Moynihan and R Bose, *Phys. Chem. Glasses*, 1972, **13**, 171.
13. W C Hasz, C T Moynihan and P A Tick, *J. Non Cryst. Solids*, 1994, **172-174**, 1363.
14. C T Moynihan, L P Boesch and N L Laberge, *Phys. Chem. Glasses*, 1973, **14**, 122.
15. C T Moynihan, *J. Non Cryst. Solids*, 1994, **172-174**, 1395.
16. J M Pochan, J J Fitzgerald and G Williams, in *Determination of Electronic and Optical Properties*, 2nd ed., B W Rossiter, R C Baetzold Eds., *Physical Methods of Chemistry Series*, Wiley-Interscience, New York, 1993, Vol. VIII.
17. A R von Hippel, *Dielectrics and Waves*, Wiley, New York, 1954.
18. A R von Hippel (Ed.) *Dielectric Materials and Applications*, Techn. Press MIT and Wiley, New York, 1954.
19. G Williams, *Chem. Rev.*, 1972, **72**, 55.
20. G Williams and J Crossley, *Ann. Rep. Phys. Chem. A*, 1977, p. 77.
21. G Williams, *Adv. Polym. Sci.*, 1979, **33**, 60.
22. G Williams in *Dynamic Properties of Solid Polymers*, NATO ASI, Eds. R A Pethrick and R W Richards, Reidel Publ. 1982, p. 213.
23. G Williams, *Trans. Electr. Insul., IEEE*, 1982, **EI-17**, 469.
24. G Williams, *Trans. Electr. Insul., IEEE*, 1985, **EI-20**, 843.
25. G Williams, in *Comprehensive Polymer Science*, eds. G Allen and J C Bevington, Vol. 2, Ch. 18, p.601, 1989.
26. G Williams, in *Structure and Properties of Polymers*, Vol. 12, of Materials Science and Technology, Ch. 11, p.471, VCH Weinheim, 1992.
27. G Williams, *Polymer*, 1994, **35**, 1915.
28. G Williams in *Keynote Lectures in Selected Topics of Polymer Science*, Ed. E Riande, CSIC, Madrid, 1995, pp 1-39 (ISBN 84-00-07472-6).
29. G Williams, in ref. 6 pp. 1-65.
30. *Relaxations in Complex Systems*, Parts I and II, K L Ngai and G B Wright, Eds., published as special editions of *J. Non Cryst. Solids*, 1991, **131-133**.
31. *Relaxations in Complex Systems 2*, Parts I and II, K L Ngai, E Riande and G B Wright, Eds., published as special editions of *J. Non Cryst. Solids*, 1994, **172-174**.
32. J D Ferry, *Viscoelastic Properties of Polymers*, Wiley, New York, 1970.
33. S H Liu, *Phys. Rev. Lett.*, 1985, **55**, 529.
34. M R Schroeder, *Fractals, Chaos and Power Laws*, Freeman, New York, 1991, p. 227.
35. S Matsuoka, *Relaxation Phenomena in Polymers*, Hanser Publ., Munich, 1992.
36. V Daniel, *Dielectric Relaxation*, Academic Press, London and New York, 1967, p. 203.
37. G Williams, *Chem. Soc. Rev.*, 1978, **7**, 89.
38. data obtained by S Baggott, G A Aldridge and the author for a high molecular weight sample of poly(vinyl acetate).
39. S W Provencher, *Comput. Phys. Commun.*, 1982, **27**, 229.
40. K Karatosos, S H Anastasiadis, A N Semenov, G Fytas, M Pitsikalis and N Hadjicristidis, *Macromolecules*, 1944, **27**, 3543.

41. H Schaefer, E Sternin, R Stannarius, F Kremer and M Arndt, *Phys. Rev. Lett.*, 1996, **76**, 2177.
42. F Kremer and M Arndt, *Dielectrics Newsletter*, April 1997, p.4 (published by Novocontrol).
43. S Havriliak and S Negami, *Polymer*, 1967, **8**, 161.
44. S Havriliak, Jr. and S Havriliak, *Dielectric and Mechanical Relaxation in Materials*, Hanser Publ., Munich, 1997.
45. G Williams and D C Watts, *Trans. Faraday Soc.*, 1970, **66**, 80.
46. G Williams, DC Watts, SB Dev and A M North, *Trans. Faraday Soc.*, 1971, **67**, 1323.
47. M F Shears and G Williams, *J. Chem. Soc., Faraday Trans. II*, 1973, **69**, 608.
48. M F Shears and G Williams, *J. Chem. Soc., Faraday Trans. II*, 1973, **69**, 1050.
49. G Williams and P J Hains, *Chem. Phys. Lett.*, 1971, **10**, 585.
50. G Williams, *Chem. Soc. Specialist Periodical Reports*, Vol. 2, Ed. M Davies, The Chem. Soc. London, 1975, p. 151.
51. N Koizumi and Y Kita, *Bull. Inst. Chem. Res.*, Kyoto University, 1978, **56**, 300.
52. A Schönhals in ref. 6, p. 81.
53. G Adam and J H Gibbs, *J. Chem. Phys.*, 1965, **43**, 139.
54. S H Glarum, *J. Chem. Phys.*, 1960, **33**, 1371.
55. R H Cole, *J. Chem. Phys.*, 1965, **42**, 637.
56. M Cook, D C Watts and G Williams, *Trans. Faraday Soc.*, 1970, **66**, 2503.
57. G Williams, *Adv. Mol. Relax. Processes*, 1970, **1**, 409.
58. G Williams in *Molecular Dynamics of Liquid Crystals*, G R Luckhurst and C Veracini (Eds.), NATO ASI, Dordrecht Publ., 1992.
59. K Araki et al., *J. Chem. Soc. Faraday Trans. II*, 1988, **84**, 1067.
60. G S Attard, K Araki and G Williams, *Brit. Polym. J.*, 1987, **19**, 119.
61. B J Berne in *Physical Chemistry, an Advanced Treatise, Vol VIII B, The Liquid State*, eds. H Eyring, D Henderson and W Jost, Academic Press, New York, 1971, p. 540.
62. E Riande and E Saiz, *Dipole Moments and Birefringence of Polymers*, Prentice Hall, New Jersey, 1992.
63. G Williams and M Cook, *Trans. Faraday Soc.*, 1971, **67**, 990.
64. C Brot and B Lassier-Govers, *Ber. Bunsenges Phys. Chem.*, 1976, **80**, 31.
65. M Baur and W H Stockmayer, *J. Chem. Phys.*, 1965, **43**, 4319.
66. K Adachi and T Kotaka, *Macromolecules*, 1988, **21**, 157.
67. K Adachi, Y Imanishi and T Kotaka, *J. Chem. Soc., Faraday Trans. I*, 1989, **85**, 1065, 1075, 1083.
68. A Schönhals in ref. 6, p. 81.
69. G S Attard, *Molec. Phys.*, 1986, **58**, 1087.
70. G Williams, *Adv. Mol. Relaxation Processes*, 1970, **1**, 409.
71. M Muller, R Stadler, F Kremer and G Williams, *Macromolecules*, 1995, **28**, 6942.
72. A S Nowick and B S Lim, *J. Non Crystl. Solids*, 1994, **172-174**, 1389.
73. G N Greaves and K L Ngai, *J. Non Cryst. Solids*, 1994, **172-174**, 1378.
74. A K Jonscher, *Nature*, 1977, **267**, 673.
75. M Meyer, P Maas and A Bunde, *J. Non Cryst. Solids*, 1994, **172-174**, 1292.
76. K Funke, *J. Non Cryst. Solids*, 1994, **172-174**, 1215.
77. M Forsyth, V A Payne, M A Ratner, S W de Leeuw and D F Shriver, *Solid State Ionics*, 1992, **53**, 1011.
78. W H Meyer, *Adv. Mater.*, 1998, **10**, 439.
79. K L Ngai in *Non-Debye Relaxations in Condensed Matter*, eds. T V Ramarishnan and M Raj Lakshoni, World Scientific, Singapore, 1987, p. 23.
80. W Götze and L Sjögren, *Rep. Progr. Phys.*, 1992, **55**, 241.
81. W Götze in *Liquids, Freezing and the Glass Transition*, eds. D Levesque, J P Hansen and J Zimm-Justin, Elsevier, New York, 1991.
82. G Williams and J Fournier, *J. Chem. Phys.*, 1996, **184**, 5690.
83. D R Baghurst and D M P Mingos, *Chem. Soc. Rev.*, 1991, **20**, 1.
84. C Gabriel, S Gabriel, E H Grant, B S J Halstead and D M P Mingos, *Chem. Soc. Rev.*, 1998, **27**, 213.



For more information on Novocontrol Dielectric measurement systems, applications or service, please call your local Novocontrol sales office.

| Factory and Head Office | |
|--|--|
| <p>Germany:</p> <p>NOVOCONTROL GmbH Obererbacher Straße 9 D-56414 Hundsangen / GERMANY</p> <p>Phone: ++(0) 64 35 - 96 23-0 Fax: ++(0) 64 35 - 96 23-33 email novo@novocontrol.com WWW http://www.novocontrol.com</p> | <p>Editor Application Notes Dr. Gerhard Schaumburg</p> <p>Abstracts and papers are always welcome. Please send your script to the editor.</p> |
| Agents | |
| <p>Benelux countries: NOVOCONTROL Benelux B.V. Postbus 231 NL-5500 AE Veldhoven / NETHERLANDS Phone ++(0) 40 - 2894407 Fax ++(0) 40 - 2859209</p> | <p>Italy: FKV s.r.l. Via Fatebenefratelli, 3 I-24010 Sorisole (Bg) Phone ++(0) 572 725 Fax ++(0) 570 507, 573 939 contact: Mr. Vanni Visinoni</p> |
| <p>Great Britain: NOVOCONTROL International PO Box 63 Worcester WR2 6YQ / GB Phone ++(0) 1905 - 64 00 44 Fax ++(0) 1905 - 64 00 44 contact: Mr. Jed Marson</p> | <p>France: Fondis Electronic Services Techniques et Commerciaux Quartier de l'Europe, 4 rue Galilée F-78280 Guyancourt Phone: ++(0) 1-34521030 Fax ++(0) 1-30573325 contact: Mr. Jean-Pierre Ellerbach</p> |
| <p>USA/Canada: NOVOCONTROL America Inc. 611 November Lane / Autumn Woods Willow Springs, North Carolina 27592 / USA Phone: ++(0) 919 639 9323 Fax: ++(0) 919 639 7523 contact: Mr. Joachim Vinson, PhD</p> | <p>Korea: HADA Corporation P.O. Box 266 Seocho, Seoul / KOREA Phone ++(0) 2-577-1962 Fax: ++(0) 2-577-1963 contact: Mr. Young Hong</p> |
| <p>Japan: Morimura Bros. Inc. 2 nd chemical division Morimura Bldg. 3-1, Toranomom 1-chome Minato-Ku Tokyo 105 / Japan Phone ++(0) 3-3502-6440 Fax: ++(0) 3-3502-6437 contact: Mr. Nakamura</p> | <p>Thailand: Techno Asset Co. Ltd. 39/16 Mu 12 Bangwa Khet Phasi Charoen Bangkok 10160 Phone ++(0) 8022080-2 Fax ++(0) 4547387 contact: Mr. Jirawanitcharoen</p> |